Available online at www.sciencedirect.com

jmr&t
Journal of Materials Research and Technology

journal homepage: www.elsevier.com/locate/jmrt

Review Article

A review of various improvement strategies for joint quality of AA 6061-T6 friction stir weldments

B.T. Ogunsemi [a,b], T.E. Abioye [c,d,*], T.I. Ogedengbe [b], H. Zuhailawati [d]

[a] Mechanical Engineering Department, College of Engineering, Landmark University,, P.M.B 1001, Omu-Aran, Kwara State Nigeria
[b] Mechanical Engineering Department, Federal University of Technology Akure, PMB 704, Akure, Ondo State, Nigeria
[c] Industrial and Production Engineering Department, Federal University of Technology Akure, PMB 704, Akure, Ondo State, Nigeria
[d] Structural Materials Niche Area, School of Materials and Mineral Resources Engineering, Engineering Campus, Universiti Sains Malaysia, 14300 Nibong Tebal, Penang, Malaysia

ARTICLE INFO

Article history:
Received 30 June 2020
Accepted 21 January 2021
Available online 29 January 2021

Keywords:
Aluminium alloys
AA6061-T6
Friction stir welding
Improvement strategies
Mechanical properties
Wear resistance

ABSTRACT

Aluminium alloys are one of the choice materials with ever-increasing demands in manufacturing industries. The aluminium alloy 6 xx series such as AA6061-T6, has emerged as one of the promising materials utilized owing to its combination of favourable properties which include high strength to weight ratio, good ductility, excellent corrosion resistance and relatively low cost. These superior properties are responsible for its emergence and usage in the fabrication of aircraft wings and fuselages, yacht/ship construction, automotive rims and wheel spacers. However, joining of AA6061-T6 including the use of friction stir welding (FSW) has serious concerns because the mechanical and tribological properties of the AA6061-T6 welded joints deteriorate significantly compared with the base metal. This phenomenon has been attributed to the severe softening encountered at the stir zone (SZ) of the aluminium matrix during FSW. Other inherent challenges of FSW such as weld thinning, kissing bond and keyhole formation also contribute to the reduction in the weld joint quality. The softening phenomenon has been linked to the dissolution of the strengthening precipitates (B″-Mg_5Si_6) as a result of high heat input during the welding process. Hence, this paper attempts to review the various improvement strategies adopted in the existing studies to improve the quality of AA 6061-T6 welded joint. These include parametric optimization, selection of appropriate tool design, pre and post heat treatments, adoption of different groove/hole designs for particle addition as well as the addition of reinforcement particles to the weld joint. The variants of FSW recently developed will also be considered. The findings from the review will generally be useful for future work on FSW of heat treated aluminium alloys. The evolution of FSW and its associated challenges are briefly discussed while the research areas yet to be harnessed are suggested for future works.

* Corresponding author.
E-mail address: teabioye@futa.edu.ng (T.E. Abioye).
https://doi.org/10.1016/j.jmrt.2021.01.070

1. Introduction

The demand for stronger, lighter and cost-effective materials for engineering applications is on the increase. Manufacturing industries, most especially the automotive and aerospace industries, continuously seek the use of materials with high strength to weight ratio, good ductility, excellent corrosion resistance and low cost [1–3]. Aluminium alloys are one of the most sought-after materials that are widely utilized in the transportation and construction industries due to their light weight, high specific strength, high toughness, corrosion resistance and recycling capabilities [4,5]. A typical grade of aluminium alloy is AA 6061 of the 6 xx series which includes Mg and Si as its major alloying elements [6]. However, in order to meet the present industrial demands which require a combination of high strength, lightness, high toughness and excellent corrosion resistance, AA 6061-T6 and some other heat-treated aluminium alloys had been discovered as promising materials that satisfy these service requirements [7,8]. AA 6061-T6 is a heat-treated, precipitation hardened aluminium alloy 6061 with specific applications in the automobile sector such as in wheel rims, wheel spacers, truck bodies, car frames and fuel tanks [9,10]. In aerospace sector, it is specifically used for making aircraft wings and fuselages and fuel tanks [11–13]. In railway sector, it is used for making container bodies, goods wagon, carriages and trams [14,15]. It also has applications in ship building and the construction of helicopter platforms [16,17]. Moreover, during manufacture or utilization of these structures, there is always a possibility or tendency of repairing defective parts which often require welding. Joining of aluminium alloys including AA 6061-T6 via conventional fusion welding processes has been reported to produce poor quality weld joints. This poor weld joint characteristics are attributed to the challenges associated with the fusion welding processes such as high tendency for solidification cracks [18,19] distortion [20], porosity and vaporization of alloying elements, which result in loss of weld strength [8]. These phenomena have been traced to high heat energy input during fusion welding processes [21–23]. As a result of these shortcomings, friction stir welding (FSW) emerged about three decades ago with a view to mitigating these possible challenges [4,18].

The term 'FSW' was invented by Wayne Thomas of The Welding Institute (TWI) in Cambridge, UK in 1991 [24,25]. It is a solid-state joining process where two or more metallic materials are intermixed mechanically and plastically deformed under mechanical pressure at elevated temperatures. The process involves a non-consumable rotating tool with specifically designed pin and shoulder [26]. The welding is accomplished by generation of heat at the abutting surfaces or joining line, as schematically shown in Fig. 1 in section 1. This is largely supported by friction between the non-consumable rotating tool and workpiece interface thereby resulting into severe plastic deformation of the workpiece [27]. More so, FSW technology has been proved to be environmentally friendly because it reduces the discharge of greenhouse gases into the atmosphere [18] in addition to its cost effectiveness [20,28]. However, the production of high quality welds of AA 6061-T61 via FSW technique has been difficult and this has led to significant deterioration observed in the tensile properties, hardness and wear resistance of the weld joints. This characteristic behaviour has been traced to the dissolution of AA 6061-T6 strengthening precipitates (β''-Mg_5S_6) which occur at elevated temperature usually above 200–250 °C [29]. Sometimes, it is referred to as loss of structural strengthening (i.e. T6 condition) at elevated temperature during FSW [30,31].

Other issues limiting the quality of friction stir welded joints (FSWed-joint) including aluminium alloys (e.g. AA 6061-T6) are insufficient pin penetration, excessive shoulder plunge depth, formation of keyholes [32–34]. Insufficient pin penetration in the FSW often results in the formation of kissing bond and other root weld flaws which are key factors limiting the strength of joints made via conventional FSW (CFSW) [35]. Excessive shoulder plunge depth, which is often caused by high tilt angle, is a major cause of weld thinning in FSW [36]. Weld thinning occurs whenever there is reduction in the thickness of the FSWed-joint relative to the other part of the weldment (i.e. base metal). According to *Zhang* et al. [36], weld thinning significantly lowers the strength of the weld joint. More so, the flexibility and wide applications of the CFSW are limited with the use backing plate. In CFSW, the use of backing plate is required to react against the high down force so as to obtain sound weld joint [34]. However, it has been established that the use of backing plate limits the utilisation of FSW in the manufacture of curved profiles and other complex-shaped structures such as hollow extrusions and rocket fuel tanks [37]. In order to overcome the shortcomings attributed to kissing bond formation, weld root flaws and use of backing plate, variants of CFSW have been developed. These variants include Bobbin tool FSW (BTFSW) [38] and tilt-probe penetrating FSW (PFSW) [35]. Unlike the CFSW which utilises only the upper shoulder, BTFSW and PFSW require the use of upper and the lower shoulders. The lower shoulder replaces the backing plate and reacts against the down force. In both variants, the pin penetrates through the entire thickness of the workpiece into the lower shoulder. With this, sufficient stirring of the material occurs from the top to the bottom of the weld joint. As a result, kissing bond and other root flaws are eliminated. Also, the use of lower shoulder increases the

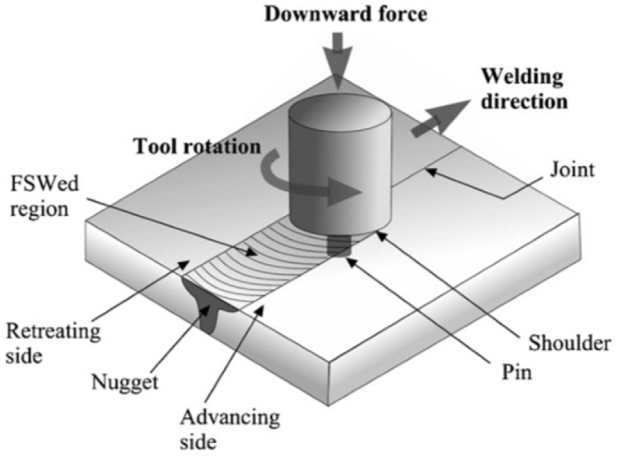

Fig. 1 – A Schematic diagram of a friction stir welding (FSW) process [69].

flexibility of the process making it possible for the fabrication of closed profiles and complex shaped structures. Unlike PFSW, the major disadvantage of BTFSW is the high tendency for pin breakage due to zero tilt angle involved in the set-up [35]. Additional pressure, which is exerted by the lower shoulder on the pin also contributes to high tendency of the pin breakage. The formation of keyholes at the end of the joint can be avoided by using retractable pin tool as identified by *Meng* et al. [39]. Also, non-weld thinning joints have been achieved successfully through the use of lower tilt angle and specially designed tool as reported by Guan et al. [33] and Zhang et al. [36]. Despite all these improvement strategies, the dissolution of the strengthening precipitates is still a major reason for poor mechanical properties in the AA 6061-T6 FSWed-joints.

Several other efforts have been made in order to improve the quality of welds produced during FSW of AA 6061-T6 aluminium alloys. These include parametric optimization of friction stir welding processes [27,40,41], analysis of the microstructure–property relationship [42,43], adoption of pre and post heat treatment [21,40,44,45] and the additions of nano and micro particles as reinforcements [21,25,44,46]. More so, the relationship between the corrosion behaviour, microstructure and mechanical properties of friction stir welded joints (FSWed-joint) of AA6061-T6 aluminium alloy have been studied [6,47]. So far, sound welds of aluminium alloys including AA 6061-T6 has been obtained using any and a combination of these improvement strategies. Also, these various improvement strategies have been largely and successfully applied in the manufacturing industries. In the light of this, this article seeks to carry out a critical review on the existing studies of some adopted improvement strategies on the microstructure, mechanical, and wear resistance properties of friction stir butt welded joints of heat-treated aluminium alloys using AA 6061-T6 as a case study. The possible future work and prospects in this area of research are also identified and discussed at the end of the review.

2. Microstructural evolution of the AA 6061-T6

The typical microstructure of FSWed-joints comprises of three distinct zones including the stir zone (SZ), thermo-mechanically affected zone (TMAZ) and heat affected zone (HAZ). As shown in Fig. 2, the SZ is always characterised with fine grain structure because the stirring of the materials occurs mainly in this zone. Due to stirring action in this zone, the materials are subjected to severe plastic deformation leading to the occurrence of dynamic recovery and dynamic recrystallization. As a result, nucleation of new grains occurs. Hence, there is occurrence of substantial grain refinement. It is observed in Fig. 2 that the microstructure become coarser as the joint transits from SZ to TMAZ and then HAZ. This is due to the fact that the degree of stirring and plastic deformation reduces from SZ to the HAZ. The TMAZ, which is characterized with deformed grains, experiences moderate temperature and strain rates while the HAZ experiences no plastic deformation [48].

Fig. 3 shows a scanning electron micrograph of a typical microstructure of the AA 6061-T6 plate. It is obvious that the grains are large and the microstructure mainly consists of two distinct phases which are continuous aluminium alloy matrix and white contrast precipitates (β''-Mg_5S_6) well dispersed in the matrix. According Reimann et al. [48], the precipitation phase occurred as a result of the T6 heat treatment (solution heat treated, quenched and artificially aged) of the aluminium alloy. This is the main strengthening mechanism in the AA 6061-T6 alloy. However, when the AA 6061-T6 is subjected to temperature above 200 °C, for example during welding, dissolution of the strengthening precipitates occurs (i.e. loss of T6 condition). For example, FSW of aluminium alloys occurs at around 400–450 °C. Consequently, dissolution of the strengthening precipitates occurred leading to deterioration of the mechanical properties at the joint. Although substantial grain refinement occurs, the loss of mechanical strength is an indication that the precipitation of the strengthening phase is the main strengthening mechanism in the AA 6061-T6. The degree of mechanical loss is a function of the amount of the dissolution of the precipitates (β''-Mg_5S_6) that occurs. The microstructure of AA 6061-T6 joints fabricated by CFSW and underwater FSW have been investigated by Fathi et al. [43] using transmission electron microscopy (TEM), as shown in Fig. 4. It was discovered that the precipitation phase (white contrast), which was identified as β''-phase, is of higher number density and well dispersed in the joint formed using underwater FSW. This is an indication that the joint formed with underwater FSW experienced lesser dissolution of the strengthening precipitates because heat was quickly extracted from the joint by the underwater. Also, the TEM analysis revealed that the dislocation density, which enhances solid solution strengthening, is higher in the underwater FSWed-joint. This is the reason for higher hardness and tensile strength demonstrated by the joints fabricated via underwater FSW.

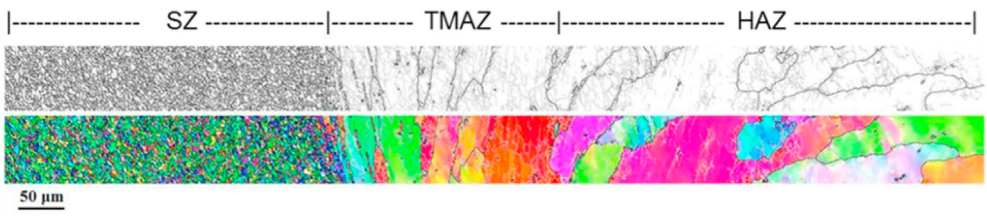

Fig. 2 – EBSD Mapping showing the degree of grain refinement in the stir, thermo-mechanically affected and heat affected zones of the AA 6061-T6 FSWed-joint [49].

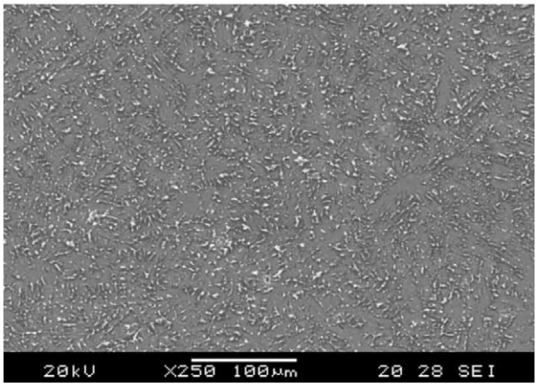

Fig. 3 – A scanning electron micrograph of a typical microstructure of the AA 6061-T6 plate.

3. Parametric optimization approach

FSW involves complex movement of material and plastic deformation via mechanical operation of a rotating tool. The rotating tool is a wear resistant high strength steel consisting of a shoulder and a pin, designed to perform mechanical stirring of the plasticized material. The stirring mechanism coupled with the movement of the tool results in severe plastic deformation of the aluminium alloy across the joining line. The quality of the joint produced is often influenced by the appropriate selection and combination of the FSW parameter [50]. The FSW process parameters established to have significant impact on the weld quality include the tool rotational speed [10,40,43], traverse speed [10,44,51–53], axial force [10,27], tool pin profile [40,41,51], plunge depth [27,43], tool tilt angle [8,18,25,27,29,52,54]. These welding parameters play vital roles in determining the weld joint characteristics. Some statistical tools including Taguchi techniques and response surface methodology (RSM) have been reported as the most profound tools for analysing the effects of the various parameters and combined parameters on the microstructure and mechanical properties of aluminium alloy 6061-T6 FSWed-joint. As previously mentioned, the major issue of concern in the FSW of AA 6061-T6 is the 'softening effect' experienced at the stir zone (SZ) of welded joint. The softening effect comes into play via the dissolution of the strengthening precipitates (β''-phase) that is initiated through the generation of high heat input by the stirring and frictional actions of the rotating tool [55]. Consequently, it has become imperative to control the amount of heat input during the welding process so as to eliminate or alleviate the softening effect at the welded joint. One of the established methods or strategies of achieving this is the optimization of the FSW parameters [56,57]. Some of the parametric combinations established for optimal quality of AA 6061-T6 FSWed-joints are summarised in Table 1.

3.1. *Impact of tool rotational speed and travel speed*

According to recent studies, high tool rotational speed at low traverse speed is a significant factor responsible for the production of quality weld joints of aluminium alloys [62]. These parameters (i.e. the tool rotational speed and traverse speed) jointly influence the amount of frictional heat generated and the degree of plastic deformation induced through the mechanical stirring during FSW [52,53]. The plastic deformation brings about dynamic recrystallization (DR) which gives rise to the growth of new grains or crystals within the nugget zone. DR is a phenomenon that accompanies friction stir welding thereby influencing the microstructure and mechanical strength of the materials at the weld joint [8]. According to *Jayabalakrishnan and Balasubramanian* [63], the extent of this phenomenon strongly depends on the process temperature and the strain rate attained during plastic deformation. Dynamic recovery and DR are considered major strengthening mechanisms (i.e. grain refinement) during FSW of aluminium alloys [52]. As shown in Fig. 5, the weld zone of a friction stir welded material(s) comprises the stir zone (SZ) or nugget zone (NZ), the thermo-mechanically affected zone (TMAZ) and the heat affected zone (HAZ). Often the SZ comprises very fine grain structure compared with the base metal which is relatively coarse. The grain size increased gradually as the microstructure transits from SZ to TMAZ to HAZ and then the base metal [64,65]. The reason is that plastic deformation, caused by mechanical stirring, mainly occurred in the SZ. As a result, DR largely occurred in the SZ and its effect declines from SZ to HAZ.

Generally, a high rotational speed often causes increased stirring per unit time while low traverse speed causes increased stirring per unit length of workpiece [66]. Now, a combination of high rotational speed and low traverse speed brings about increased stirring of a unit length of workpiece per unit time. Therefore, large frictional heat is generated per unit time and the plastic deformation is very much severe, leading to high degree of DR. Hence, substantial grain refinement is achieved and the mechanical properties of the weld joints of aluminium alloys are improved [6,67]. In the case of AA 6061-T6, care must be taken because excessive heat generation will cause the dissolution of the strengthening precipitates (β''-phase) which is the major strengthening mechanism in the alloy. Due to this, the parameters (i.e. rotational speed and traverse speed) should be optimized so that the dissolution of the strengthening precipitates (i.e. softening effect) is minimized and the effect of grain refinement is achieved [6,8,52,68]. Significant improvements in the hardness, impact strength and tensile strength of the weld joints relative to the base metal that meet the specifications of various manufacturing industries including aerospace, automotive, marine etc. have been achieved through optimization of the process parameters. For example, *Safeen* et al. [60] has achieved a hardness of 95%, tensile strength of 92% and impact strength of 87% of the base metal through parametric optimization. Also, 67% tensile strength of the base metal has been achieved by *Elatharasan and Senthil-Kumar* [69] through parametric study of AA 6061-T6 FSW.

It has been found that increasing the welding speed for AA 6061-T6 FSW would decrease the heat generation in the joints [70]. Therefore, there is a reduction in the loss of structural strengthening associated with Mg_2Si precipitates [6,52,68]. On the other hand, excessive tool rotational speed is also a critical factor, which causes the softening effect along the joining line. Therefore, the rotational should not be extremely high

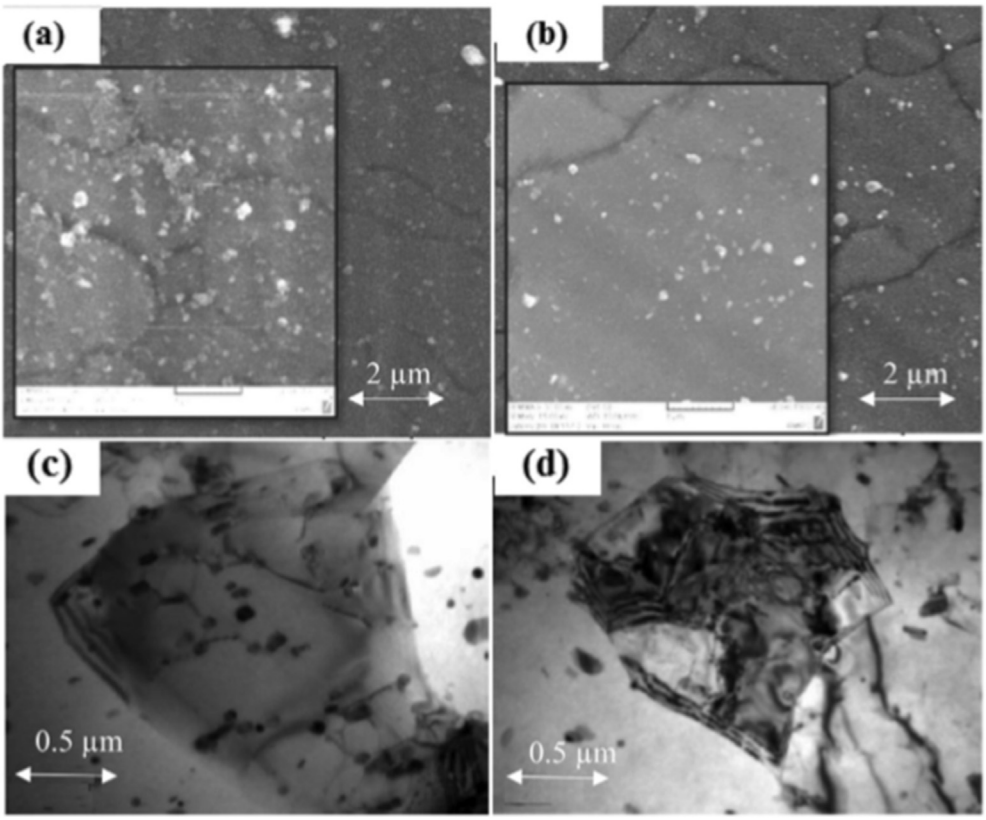

Fig. 4 – SEM micrographs showing the strengthening precipitates dispersion of the joint fabricated by (a) underwater FSW and (b) Conventional FSW, and TEM micrographs showing the dislocation formed in (c) underwater FSW and (d) conventional FSW [43].

and the traverse speed should not be extremely low during the FSW of AA 6061-T6 so as to obtain high quality weld [12,67,71,72]. Based on the past work, the optimal values of the rotational speed and traverse speed for the FSW of AA 6061-T6 are 800–1200 rpm and 40–90 mm/min respectively [4,49,55,73–77]. For example, Gharavi et al. [6] reported that FSW of AA 6061-T6 using tool rotational speed ranging from 800 to 1200 rpm at low welding speed of (<40 mm/min) resulted into increased tensile strength and hardness. However, reduction in hardness could be observed whenever the traverse speed exceeds 90 mm/min for the range of maximum rotational speed earlier mentioned [70]. More so, statistical studies detailing the significant effect of each of the parameters on the mechanical properties of AA6061-T6 FSWed-joints has been a subject of investigation by many researchers [10,52,53]. Results from various parametric (statistical analysis) studies on FSW of aluminium alloys indicated that the tool rotational speed has the maximum percentage contribution to the enhancement of the mechanical properties such as the tensile strength, hardness and wear properties of friction stir welded AA6061-T6 [10,53].

3.2. *Impact of tool geometry*

Tool geometry is one of the important factors considered to be responsible for the production of high quality FSWed-joints. This is because it governs the frictional heat generation during mechanical stirring action required to join the aluminum alloy(s) effectively [50]. However, the tool profile is also noted as one of the predominant factors that influence the joint strength of AA 6061-T6 along with other process parameters such as the tool rotational speed and travel speed [78]. The profile of the tool controls to a large extent the material mixing, flow, temperature as well as formation of different zones. The heating rate, plastic flow, forging pattern of the weld region as well as the morphology are determined, to some extent, by the tool design or geometry. These consequently influence the joint quality of the FSW welds [40,79]. The tool geometry consists of a shoulder and a pin. Both serve the primary purpose of inducing localized heating, material mixing and flow [80, 81]. Tool geometries or configurations have been studied extensively and established to have exerted significant effect on the material flow and the resulting weld properties of FSWed-aluminum alloys 6 xx series. The utilization of appropriate or suitable tool profile or design, with the combination of optimum process parameters, is considered most significant in the realization of high quality FSWed-joint [68]. The tool pin geometries considered in previous studies include the hexagonal [79] square [43,62], cylindrical threaded [8,40,71], pentagonal, cylindrical and tapered cylindrical [50], conical and conical threaded [82,83], trapezoidal and cylindrical grooved [78,84]. Each tool profile, some of which are presented in Fig. 6, moves the plasticized material in different ways.

Table 1 – A summary of some established parameters at which high quality friction stir weldments of AA 6061-T6 and other heat-treated aluminium alloys were achieved.

S/N	Materials used	Process Parameters	Plate Thickness	Tool Material/Geometry	Outcome/Findings	Ref.
1	DissimilarAA6061-T6 and AA2024-T351 reinforced with SiC particles at the joint	Rotational speeds: 800 rpm; welding speeds: 31.5 mm/min; Tool offset: 0.5 mm; Groove width: 0.3 mm. Pre-weld annealing was performed at 415 °C for 2 h and then cooled in furnace. Post–weld artificial aging was done by first solution heat treated at 530 °C for 70 min and then artificially aged at 190 °C for 18 h.	6 mm	H13 steel (square frustum probe). Shoulder diameter:18 mm with a 4° conical cavity; Probe diameter: 3.5–7 mm; Probe Length: 5.9 mm.	The pre annealing and post aging heat treatment resulted in tensile strength and toughness of 92 and 96% of AA6061-T6 tensile strength and toughness, respectively	[21]
2	AA 6061-T6 - AA 7075-T6	Rotational speeds: 450, 560, 710, 900 rpm; Welding speeds: 25, 31.5, 50, 80 mm/min; Tilt angle: 2.5°; Shoulder plunge depth: 0.3 mm	5 mm	AISI H13 Steel with Taper Cylindrical Threaded Pin. Pin diameter: 6 mm; Shoulder diameter:30 mm;	The maximum ultimate tensile strength was obtained at 560 rpm and 31.5 mm/min with or without nanoparticles. The lowest residual stress and highest yield strength were also achieved at this condition.	[25]
3	AA6061-T6	Rotational Speed: 900 rpm; Travel Speed: 1.25 mm/s	6 mm	H13 Steel (Taper and taper threaded tools). Shoulder diameter: 18 mm; Pin diameters (top and bottom): 6 mm and 3 mm respectively.	Better tensile properties were achieved in the FSW samples produced with the taper-threaded-pin tool. The tensile properties of samples obtained by using taper threaded-pin tool were discovered to increase with tilt angle.	[27]
4	AA6082-T4	Rotational Speed: 600 rpm; Welding Speed: 400 mm/min	2.85 mm	Tool inner and outer shoulders (Concave). Plunge depth of inner and outer shoulders: 0.15 mm and 0.05 respectively.	Elimination of flash defects as weld-thinning was avoided. The UTS obtained was 231 MPa, which was 91% that of the base metal (BM).	[33]
5	AA 6082-T6	Rotational speed: 800 rpm; Welding speed: 10–200 mm/min.	5 mm	A self-support tool with double shoulder (a concave upper shoulder and the smaller convex lower shoulder). Upper shoulder diameter: 14 mm; Lower shoulder diameter: 9 mm pin length: 4.6 mm.	It was inferred that the welding speed played a significant role during self-support FSW (SSFSW). The tensile strengths of the SSFSW joints were found to increase with the welding speed as the maximum tensile strength achieved was equivalent to 69% of that of the parent metal.	[38]
6	AA6061-T6 reinforced with B4C particle	Welding speed: 50–400 mm/min; Rotational speed:1000 rpm	2.9 mm	Threaded Cermet Pin (conical); Pin root diameter: 5 mm, Taper ratio: 6; Pin length: 2.8 mm; Shoulder diameter:14 mm	The joint quality increased significantly with increasing welding speed, giving a joint efficiency of ~70% at 400 mm/min.	[58]
7	*DissimilarAA6061-T6 and AA2024-T351 reinforced with SiC particles at the joint*	Rotational speeds: 800 rpm; welding speeds: 31.5 and 40 mm/min; Tool offset: 0, 0.5, 1 mm; Groove width: 0, 0.2, 0.3 and 0.4 mm	6 mm	H13 steel (square frustum probe). Shoulder diameter:18 mm with a 4° conical cavity; Probe diameter: 3.5–7 mm; Probe Length: 5.9 mm.	Most uniform particle distribution and optimal mechanical performance were found at the groove width 0.3 mm, tool offset 0.5 mm towards the AA6061-T6 side with rotational speed 800 rev min^{-1} and travel speed 31.5 mm min^{-1}.	[59]

8	AA 6061-T6	Rotational speed: 850–1450 rpm; Welding speed: 30–110 rpm; Tilt angle: 1 - 4°; Tool profile: simple cylindrical (SC), cylindrical with threads (CT), simple tapered (ST), tapered with threads (TT), and simple square (SS)	5 mm	Molybdenum-based high-speed steel. Shoulder diameter:18 mm with a 6° conical cavity; Pin diameter: 6 mm; Pin Length: 4.7 mm. The pin base and tip diameter for ST and TT were 6 and 4 mm, respectively.	Maximum UTS, hardness and impact toughness which are respectively 92%, 95% and 87% of the base metal were achieved at 1150 rpm rotational speed, 70 mm/min welding speed, 3° tilt angle and simple cylindrical pin profile.	[60]
9	AA6061-T6	Rotational Speed: 900 rpm; Welding Speed: 98 mm/min; Plunge Depth: 5.9 mm	6.1 mm	H13 Die Steel (cylindrical grooved, CG; cylindrical grooved with flutes, CGF; cylindrical full threaded, CFT; cylindrical full threaded with flutes, CFTF; cylindrical half threaded, CHT; square, SQ; and cylindrical tapered, CT; tool pin	It was observed that homogenous microstructure and finer grains were relatively found within the stir zone (SZ) for joints produced using CGF and CG tool pins. Also, the Ultimate Tensile Strength (UTS) and flexural load were highest for joints prepared using CGF and followed by CG tool pin as compared to other pin geometries.	[61]

The processes involved in friction stir processing (FSP) and FSW are similar. FSP is applied for enhancing surface properties while FSW is for joining two materials together. Pin volume ratio (i.e. dynamic volume of pin/static volume of pin) has been established to be a significant parameter influencing the actual stirring action and material consolidation during FSP of AA 6061 [85]. As a result, *Vijayavel and Balasubramania* [86] has investigated the effect of pin volume ratio of four different tool pin profiles, namely, straight cylindrical (STC), tapered cylindrical (TAC), threaded cylindrical (THC) and tapered threaded cylindrical (TTC) during the FSP of aluminium based metal matrix composite. Compared with others, FSP region produced with the tapered threaded cylindrical (TTC) exhibited superior hardness and tensile properties. Also, the ultimate tensile strength, yield strength and percentage elongation of AA 6061-T6 weldments, irrespective of the tilt angles, produced by (i) tapered-pin tool and (ii) taper-threaded-pin tool has been a subject of investigation by *Banik* et al. [27]. Better tensile properties were achieved in the FSW samples produced with the taper-threaded-pin tool. The findings or facts that tools with tapered threaded pin usually yield friction stir welds with enhanced mechanical properties have been supported by several other researchers [25,45,50,84]. The improved weld joint properties (e.g. hardness, tensile properties) associated with the use of the tapered threaded pin tool also has been attributed to the enhanced material movement, which is often aided by the threads from the root weld to the top of the weld. However, the quality of the joint has also been established to be influenced by the pitch of the thread [83]. If the thread pitches are too large (for example 3.81 mm and beyond), too much material may escape from the root weld as flash therefore causing some defects like tunnel and wormholes near the root of the weld [83]. Research on the use of hexagonal pin tool revealed that the use of this type of tool geometry enhances high frictional heat generation (through improved stirring), which aids DR and dynamic recovery [79]. These two phenomena produce substantial grain refinement in aluminium alloy FSWed-joints. Hence, joints of improved tensile and hardness properties have been produced using hexagonal tool pin compared with the conical, tapered, triangular and squarely shaped pin tools [79]. In FSW, lifting of workpiece often occur whenever the workpiece is not firmly clamped to the backing plate and when the tool is not quickly retracted from the workpiece after the FSW process. This challenge can be overcome by ensuring firm clamping of the workpiece and quick retraction of the tool from the workpiece immediately after welding.

3.3. *Impact of tool tilt angle*

The tool tilt angle is considered one of the vital parameters that contribute significantly to the quality of FSWed-joints [27]. The mechanical and microstructural behaviours of 6 xx series aluminium alloys such as AA6061-T6, had been studied by varying the tool tilt angles. Several studies have been carried out to establish the appropriate tilt angles at which enhanced mechanical properties of AA6061-T6 can be achieved while utilizing different tool pin designs. Till date, the tool tilt angles adopted by researchers for friction stir welding of AA6061-T6 have been between 0° and 3°. This assertion was

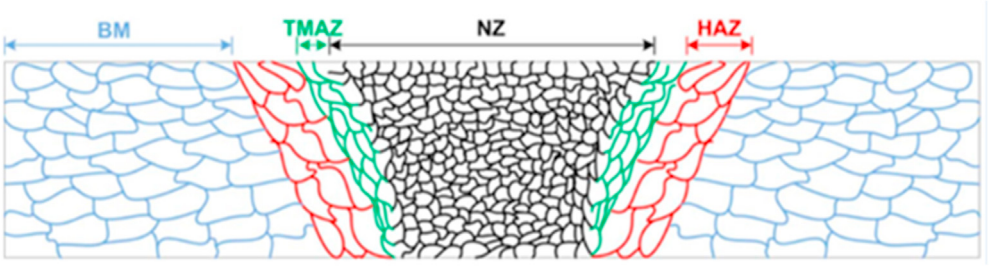

Fig. 5 – Schematic showing different zones in a cross-sectioned FSWed-joint [64].

confirmed from the studies conducted by [29] 2° [52], 1° [27], 0° 1.5° 3° [54], 3° [25], 2.5° [8], 2.5° [46], 2.5° [18], 2.5° [6], 3° and [80] 2.5°. However, some of the literature established that 0° tilt angle is always associated with the occurrence of weld defects such tunnel and poor surface finish [27,87]. Recent studies revealed that increasing the tool tilt angles from 1° to

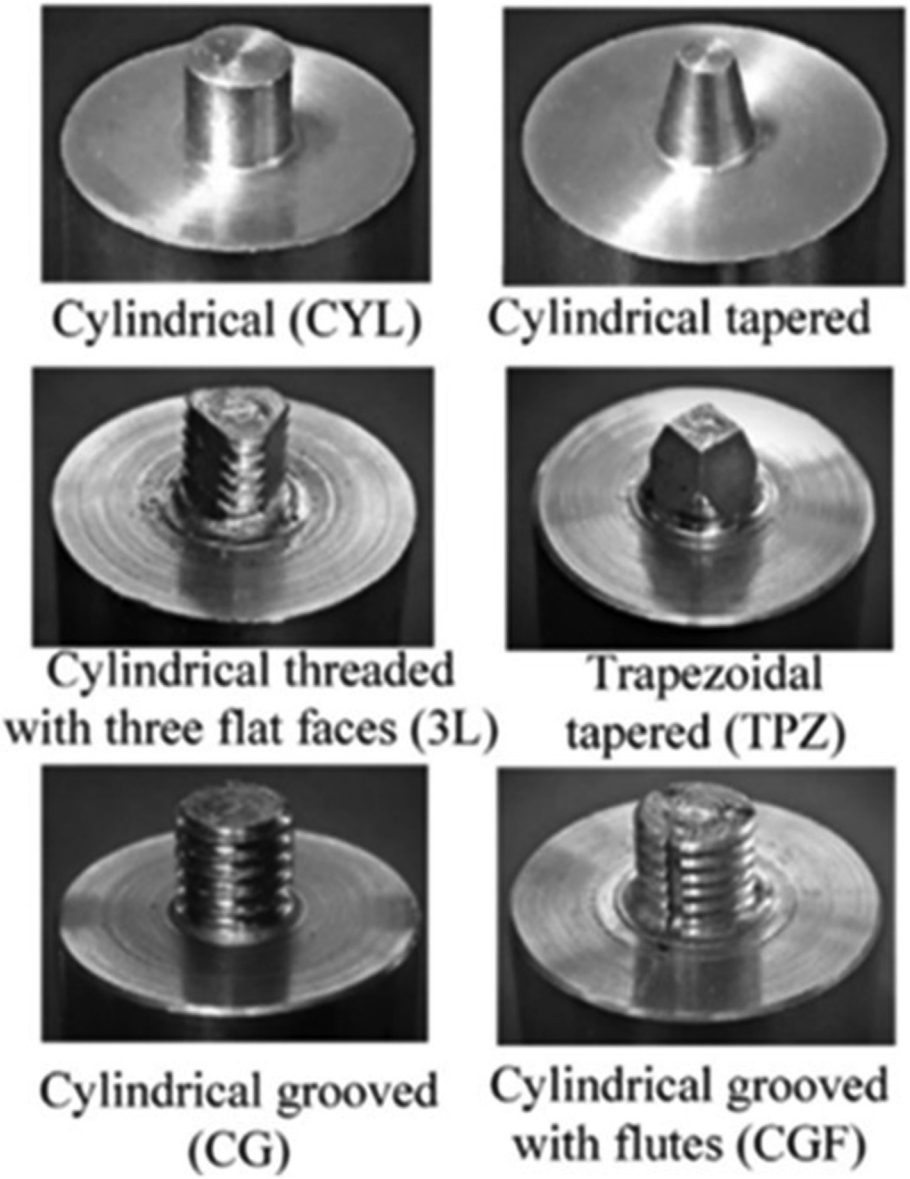

Fig. 6 – Images of different tool profiles utilised in FSW process [40].

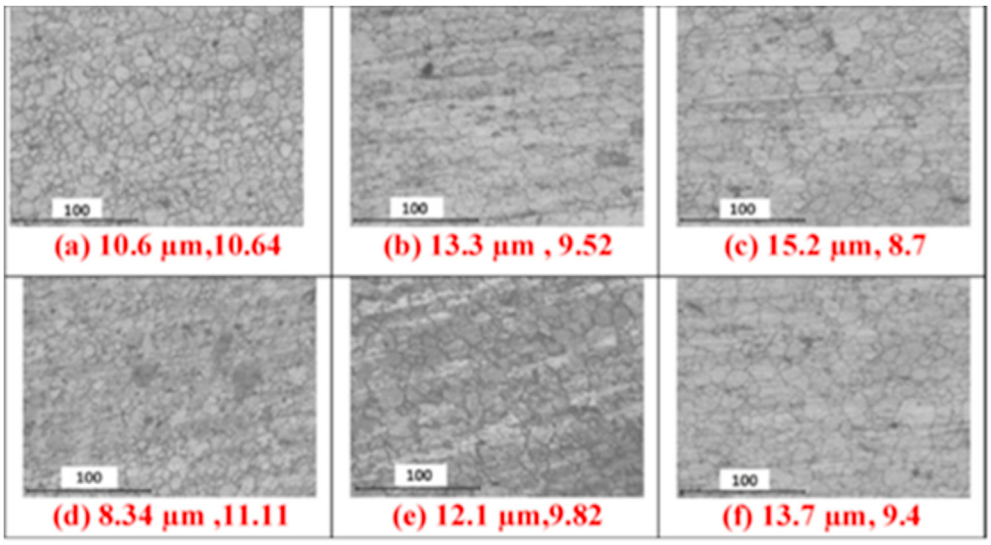

Fig. 7 – Grain sizes and grain numbers at the stir zones formed at varying tilt angles for taper and taper-threadedtool (a) TT 0° (b) TT 1 degree° (c) TT 3° (d) TTH 0° (e) TTH 1.5° (f) TTH 3° [27].

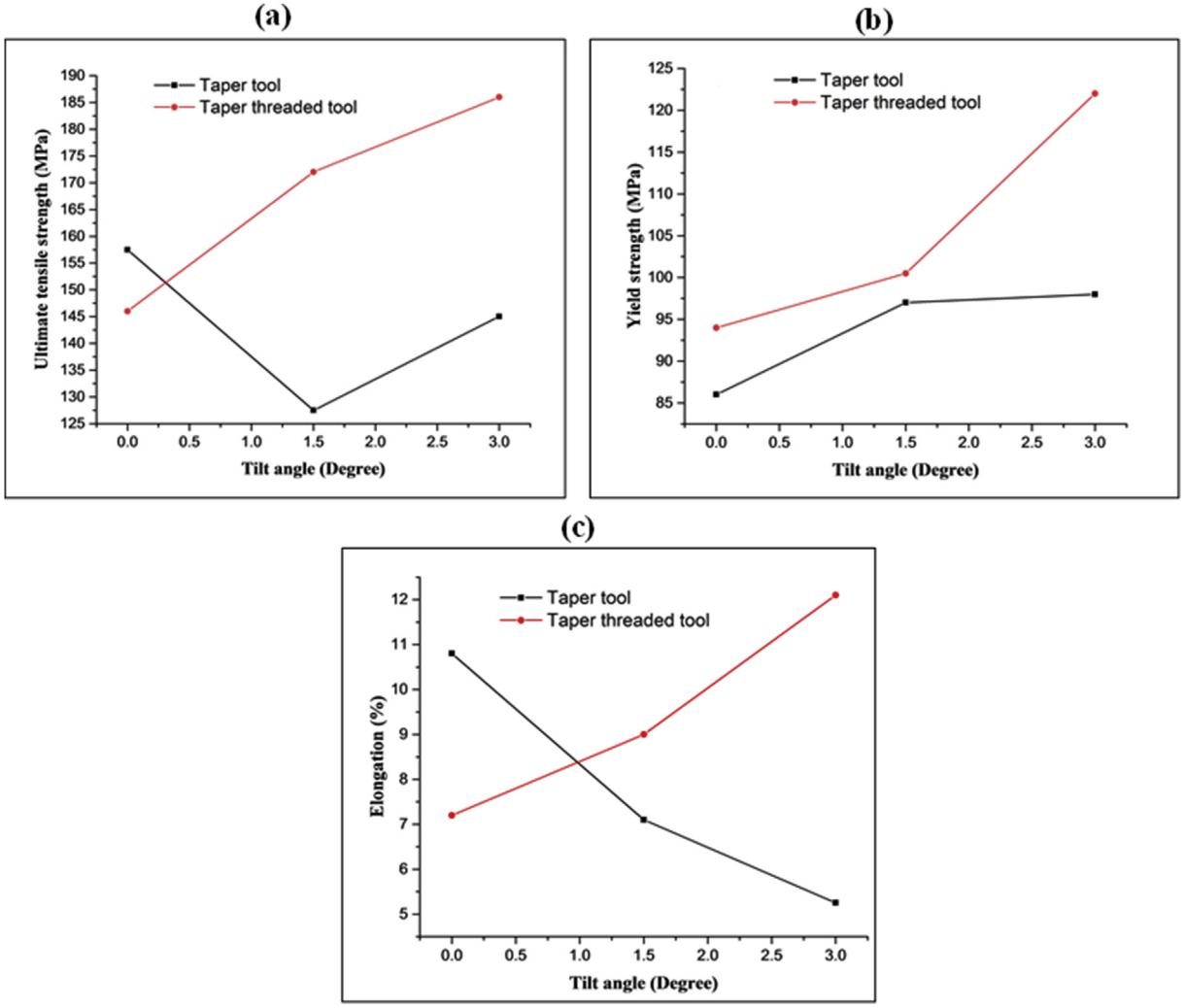

Fig. 8 – (a) Ultimate tensile strength (b) yield strength (c) % elongation of AA 6061-T6 friction stir weldment at varying tilt angles [27].

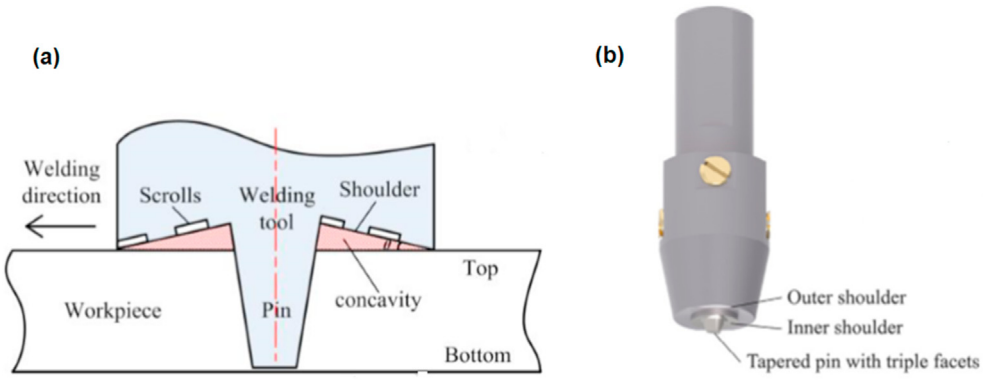

Fig. 9 – Non-Weld thinning FSW specially designed tools (a) with concave shoulder having incorporated equally spaced scrolls [36] and (b) having inner and adjustable outer shoulder [33].

3° results in the accumulation of higher volume of material or material clustering under the tool shoulder. This further results in an increase in the torque and other forces associated with FSW as the tool tilt angles increase [27]. The implication of this is that 1° tilt angle will produce finer grain structure when compared with the grain structure formed with 3° tilt angle (as presented in Fig. 7). According to Banik et al. [27], the hardness, yield strength and tensile strength of AA6061-T6 friction stir weldment increased with increasing the tilt angle, for tapered-threaded pin tool (see Fig. 8). Unlike the ordinary tapered tool, the tapered threaded pin tool profile forces the low viscous plasticized material to rise or climb through the threaded pin pitch, which acts as a channel for material movement. As a result, the tapered threaded pin tool (unlike unthreaded pin tool) can effectively promote the mixing of materials and also enlarge the material flow zone for improved tensile properties and enhanced hardness. The increase in the tensile can also be attributed to the iron-aluminium phase formation due to the accumulation of iron element under the tool shoulder as the tilt angle increased to 1.5° and 3°. In the case of tapered pin tool, the tensile properties do not follow any particular pattern but the highest tensile properties were achieved at 3° tilt angle. However, it should also be noted that for samples welded using tapered-pin tool at 1.5° and 3° tilt angles as well as taper-threaded tool at 0° tilt angle, large peak of iron were observed beside the peak of Al, Mg and Si. Also, inclusions of several foreign particles in the order of several micro-meters in size are also noticeable from the EDS spectrum. Consequently, the optimum tilt angle at which enhanced mechanical properties of AA6061-T6 can be achieved for both tapered, threaded and unthreaded taper tools has been established to be between 1.5 and 2.5° [8,18,25,80,88].

However, it has been established that high tilt angle usually results in excessive shoulder plunge depth, which is the main cause of weld thinning in friction stir weldments. As previously mentioned in section 1 of this paper, weld thinning reduces the strength of the FSWed-joint. Several efforts have been utilised to overcome the weld thinning defect in FSWed-joints. The use of stationary shoulder has been tried and the welding efficiency is not satisfactory [89]. Also, addition of more solid-state material along the weld joint line during the FSW of two butted workpieces have been tried [90]. The major deficiency of this is that the joints are always higher than the other parts of the weldment therefore requiring the machining of the welded joint so that it can be in the same plane as the base metal. This makes the process complicated and less efficient. However, non-weld thinning FSWed joints can be efficiently produced through the use of specially designed tool. According *Zhang* et al. [36], zero shoulder plunge depth can be achieved by using a tool having concave shoulder with equally spaced scrolls incorporated on the inner surface of the concave shoulder, as illustrated in Fig. 9a. Compared with the weldment made with CFSW, weldment produced via this specially designed tool showed better grain refinement as well as improved tensile strength [56]. More so, the fracture location of the joint fabricated via this specially designed tool moved towards the weld centerline in contrast to C-FSW joint. Non-weld thinning FSWed-joint has also been successfully achieved by *Guan* et al. [33] by using a special tool made of inner shoulder and adjustable outer shoulder as shown in Fig. 9b. In this design, the outer shoulder can be adjusted to control the protrusion of the inner shoulder relative to the outer shoulder. The outer shoulder accumulates and refills the overflowing materials so as to eliminate weld thinning defect. This arrangement was utilised for 2.85 mm thick AA 6068-T4 and maximum tensile strength up to 91% of the base metal was achieved [33].

4. Reinforcement additions during FSW of AA 6061-T6

In recent times, particulate reinforcement additions have gained a lot of research focus as one the improvement strategies adopted for enhancing the mechanical properties of AA 6061-T6 friction stir welded joints. The additions of various reinforcement particles as one of the techniques for improving the mechanical performance of FSWed-joints of AA 6061-T6 have been reported [46,56]. From the existing studies, the effects of the additions of SiC, Al_2O_3 (Alumina) and B_4C nanoparticles [46], SiO_2 nanoparticles [25], SiC [21,29], Al_2O_3 nanoparticles [7], carbonaceous micro particles such as graphite, carbon nanotubes and graphene [91] and copper

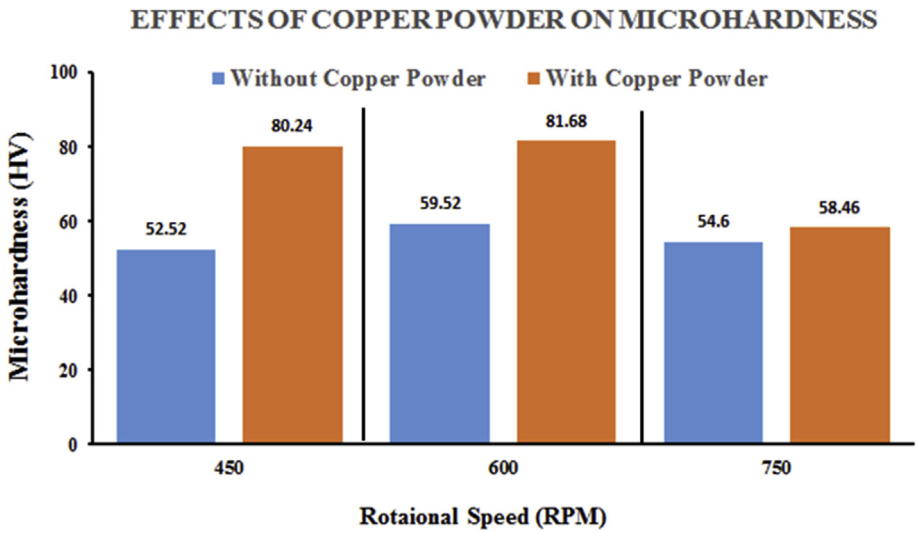

Fig. 10 – Effects of copper powder on micro hardness AA 6061 friction stir welded joint at different rotational speed reproduced from [56].

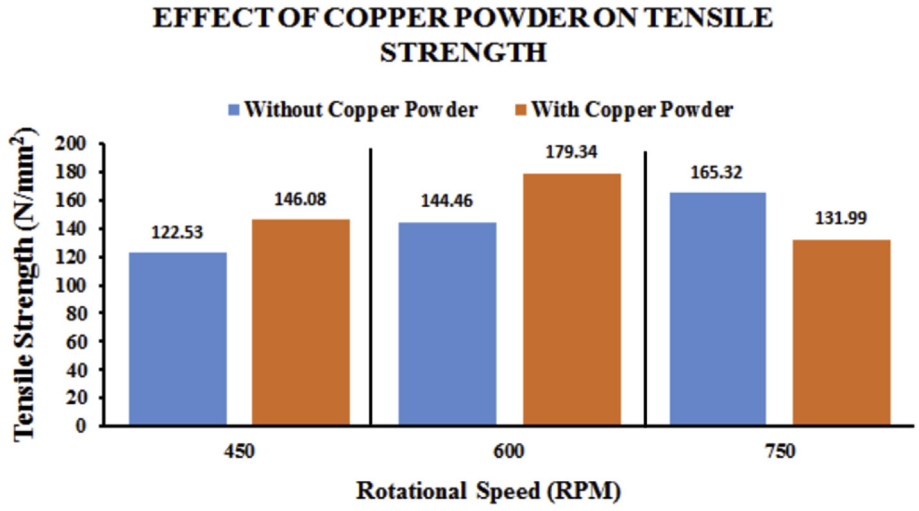

Fig. 11 – Effect of copper powder on tensile strength AA 6061 friction stir welded joint at different rotational speed [56].

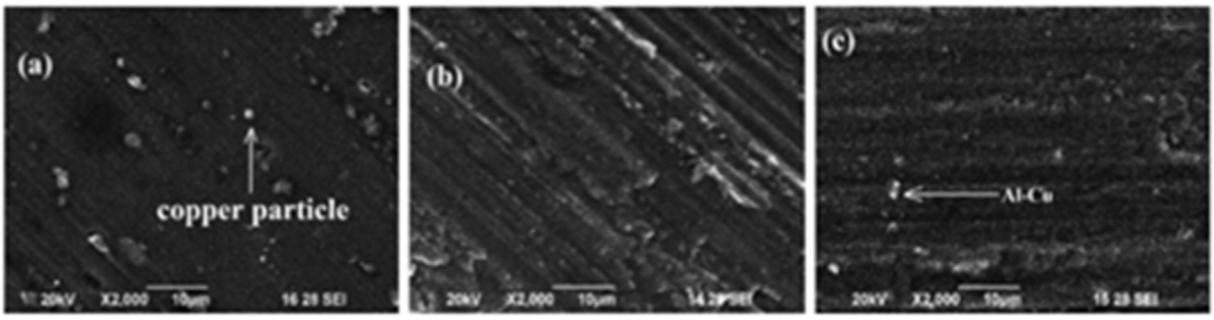

Fig. 12 – SEM micrographs showing copper particle dispersion in AA 6061 friction stir welded joint (a) 450 rpm (b) 600 rpm (c) 750 rpm [56].

Table 2 – Overview of the effects of reinforcement additions on the quality of AA 6061-T6 friction stir welded joints/processed surfaces.

S/N	Type of Particles used	Particles Sizes	Utilised Process Parameters	Number of Passes	Remark/Findings	Ref.
1	Al_2O_3	15 nm	2000 rpm; 70–80 mm/min	Single	The reinforced sample has UTS of 250 MPa as compared to the unreinforced sample with 200 MPa.	[7]
2	Cu Powder	20 μm	660 rpm; 63 mm/min	Double	A maximum tensile strength of 180 MPa was achieved for the Cu-reinforced FSW joints.	[20]
3	SiC	20 μm	1400 4pm; 50 mm/min	Single	A maximum hardness of about 116 HV was achieved by the reinforced sample.	[30]
4	SiC, Al_2O_3, B_4C	3–15 μm	850 rpm, 45 mm/min	Single	B_4C, Al_2O_3 and SiC reinforced joints showed improvements of about 42%, 34% and 22% over unreinforced joint which has hardness value of 65 HV. The reinforcement additions reduced the wear rate of the welded joint by up to a factor of ~1.7 and ~1.9 at 30 N and 50 N load conditions respectively.	[37]
5	Cu Powder	30 μm	450,600,750 rpm; 44 mm/min	Single	Cu-reinforced joint shows hardness of 81.68 HV and UTS of 179.34 MPa while the unreinforced joint exhibited hardness of 59.5 HV and UTS of 144.41 MPa	[45]
6	B_4C	7 μm	1000 rpm, 50–400 mm/min	Single	The highest joint efficiency of ~70% was exhibited by the reinforced sample. After, aging, the joint efficiency was improved and increased to ~85% for the reinforced joint produced at 400 mm/min.	[70]
7	(SiC + Gr) and (SiC + Al_2O_3)	20 μm	900,1120,1400 rpm	Single	Maximum tensile strength of at 900 rpm is 219 MPa was achieved at 900 rpm which is close to the value found for the base metal (265 Mpa)	[76]
8	Cu + SiC		710,1000,1400 rpm; 50,63,80 mm/min	Single	Reinforced joint efficiency of 96% was achieved for 1000 rpm/80 mm/min. This provides a major improvement over the unreinforced welded joint	[92]
9	SiC	60 nm	550,600,650 rpm; 25 & 35 mm/min	Single	At 650 rpm and 35 mm/min, the reinforced sample exhibited 28% improvement in tensile strength as compared to the unreinforced joint. The mean micro-hardness of reinforced sample is greater than that of the unreinforced sample.	[93]
10	B_4C	5–7 μm	1200 rpm; 100 mm/min	multi-pass	The reinforced surface showed a higher average hardness of 98 HV as compared to the unreinforced sample (53 HV). Increasing the number of passes led to homogenous dispersion of particles within the stir zone	[94]
11	SiC + Gr	20 μm	650 rpm/3.4 m/s	Single	The wear rate at optimum condition decreased. The presence of Gr decreased the wear rate because it acted as solid lubricant. Micro-hardness at optimum condition increases due to the presence and pinning effect of hard SiC particles.	[95]

Table 3 – Tensile test results of Cu-reinforced Friction stir welded joints of AA6061 at varying rotational speeds [105].

Rotational Speed (rpm)	Welding Speed (mm/min)	Yield Strength (N/mm^2)	Ultimate Tensile Strength (N/mm^2)	Elongation (%)	Joint Efficiency (%)
710	50	115 ± 2	175 ± 2	5.7 ± 0.1	69
710	63	136 ± 2	192 ± 2	5.5 ± 0.1	76
710	80	149 ± 2	204 ± 3	5.2 ± 0.1	80
1000	50	144 ± 3	206 ± 3	5.1 ± 0.1	81
1000	63	173 ± 2	223 ± 2	4.6 ± 0.1	88
1000	80	197 ± 2	243 ± 3	4.3 ± 0.1	96
1400	50	119 ± 3	167 ± 3	6 ± 0.1	66
1400	63	136 ± 2	183 ± 2	5.8 ± 0.1	72
1400	80	159 ± 2	204 ± 2	5.4 ± 0.1	80

powder [56] have been experimentally investigated. In all cases, the addition of these micro and nanoparticles was reported to have strengthened the FSW joint of AA6061-T6 thereby enhancing the mechanical and wear performances of the weldment. However, uniform distribution of the particles in the joint is germane to achieving enhanced mechanical and wear performances of the joint. This can be achieved through proper selection of parameters and using double or multiple weld passes.

Increasing tool rotational speed combined with the particulate reinforcement has been reported to greatly impact the micro-hardness and tensile strength of the welded joint positively (see Figs. 10 and 11). Particle clustering/agglomeration is often observed in the stir zone region as a result of reinforcement additions. However, increasing the rotational speed significantly reduces the cluster size (improve particle distribution) thereby resulting in grain refinement (as shown in Fig. 12) and improved mechanical properties.

4.1. *Effects of the particle addition on the hardness property*

According to literature, particles (micro or nano size) addition to the AA 6061-T6 welded joint has been established to show significant improvements on the hardness property of the joint [92–94]. The hardness property enhancement can be traced to (i) the pinning effect caused by the obstruction of the grain growth by the injected reinforcement particles and (ii) inherent property of each of the injected reinforcement particles. During FSW process, aluminium matrix and other materials are subjected to severe plastic deformation causing the formation of several low-angle disoriented grain boundaries. In the process, the low angle boundaries would be converted to high angle boundaries leading to the nucleation of new grains. This process is called DR. The growth or size of the new grains depends on the amount of heat generated and the cooling time [95]. However, with the addition of the reinforcement particles, the particles often act as obstacles

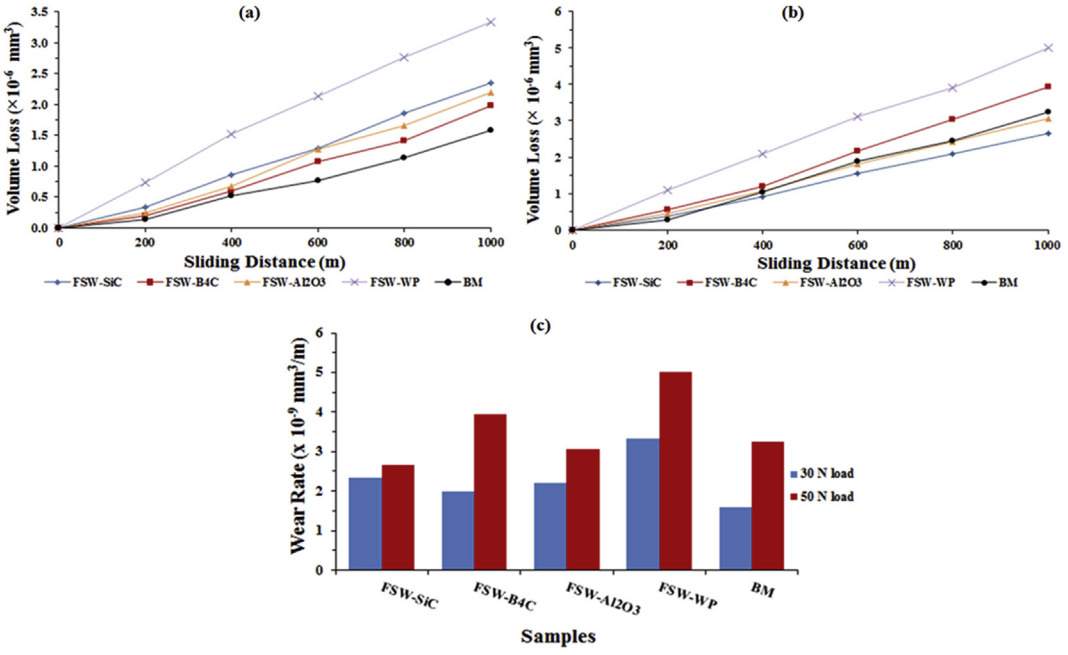

Fig. 13 – Results of wear volume loss against sliding distance at (a) 30 N load, (b) 50 N load and wear rates at both load conditions for base metal (BM), unreinforced and reinforced joints during the FSW of AA 6061-T6 [46].

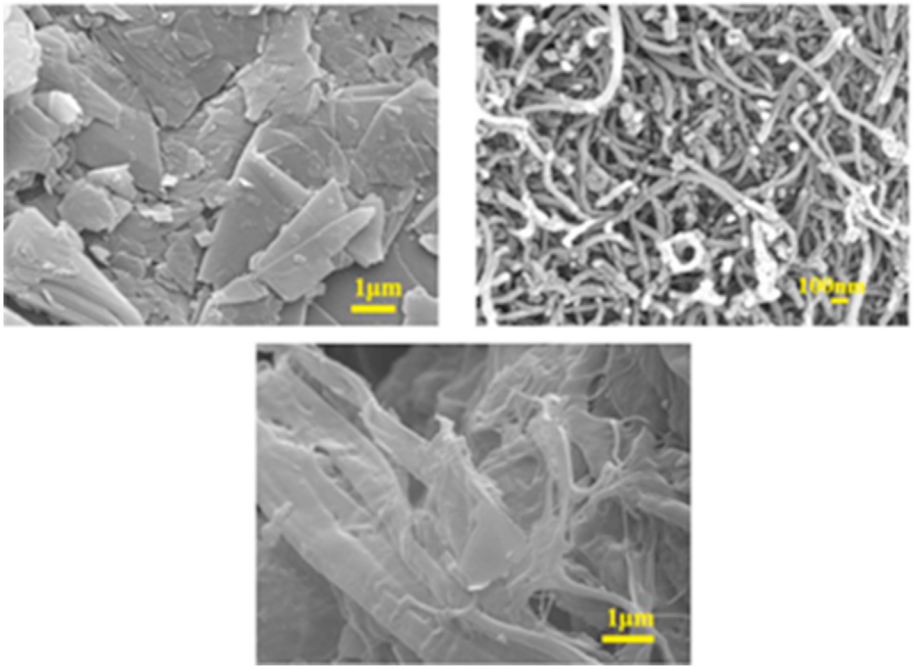

Fig. 14 – SEM micrographs showing raw carbonaceous materials; (a) graphite (b) carbon nanotubes and (c) graphene [91].

against the grain boundaries thus preventing the growth of the new grains. This is called pinning effect [96].Therefore, pinning effect enhances grain refinement. According to Hall–Petch equation, hardness increases with the reduction in the grain size [97].

Also, the inherent hardness of the reinforcement particle plays a significant role [98]. The ceramics particles are harder than the matrix alloy. Uniform distribution of these particles in the soft matrix will enhance the hardness of the matrix. Consequently, this will compensate for the hardness loss that may result from the loss of structural strengthening (T6 condition). Past work has revealed that the hardness of the reinforced AA 6061-T6 welded joints is significantly higher than that of the unreinforced joint and very close (usually > 75%) to that of the base metal [46]. This degree of improvement in hardness has been found to increase with the inherent hardness properties of the reinforcement particle added. The addition of B_4C particle (~3800 HV) has shown increased hardness of the aluminium welded joints compared with the addition of the Al_2O_3 (~2348 HV) and much better than the SiC (~2270HV) addition [46,98]. More so, the hardness property was found to increase with the increase in the particle content [31]. The particle content is often being determined by the size of the groove (or holes) machined along the

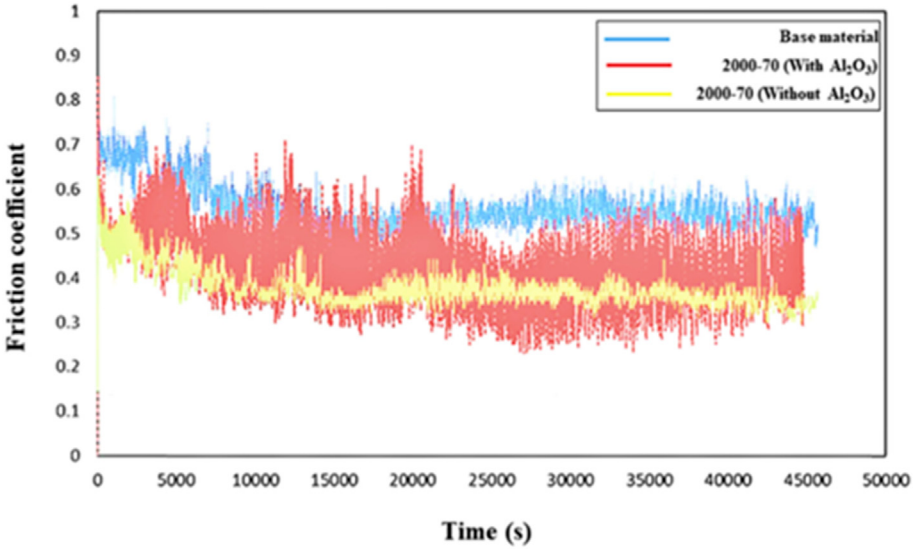

Fig. 15 – Extracted coefficient of friction patterns of unreinforced and Al2O3 reinforced AA 6061-T6 joint samples in comparison with the parent metal reproduced from [7].

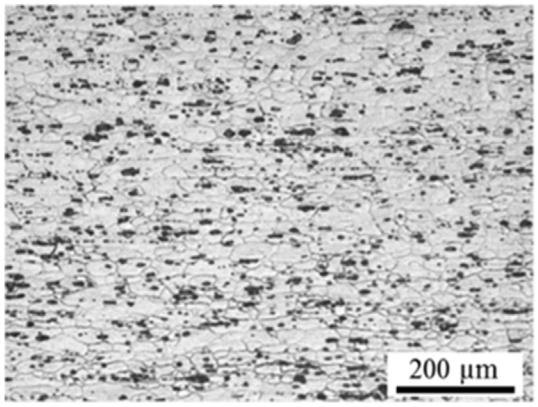

Fig. 16 – Microstructure of the as-received AA6061-T6 [4].

adjoining edges of the workpiece before the welding process. The particle content varied directly with size of the groove. However, if the groove size is beyond a threshold, usually 2 mm width [20], there is high tendency that the joint will be characterized with defects such as tunnels and poor surface finish. As a result, the hardness property may decline.

Increasing tool rotational speed in addition to the particulate reinforcement has been reported to greatly impact the micro-hardness of the welded joint positively (see Fig. 10) [56,93]. As previously mentioned in this work, high rotational speed at low traverse speed results in high heat input, which enhances material flow around the tool pin and eventually produce severe plastic deformation. Due to the improved materials flow, reinforcement particle distribution is more uniform. Also, substantial grain refinement resulting from both severe plastic deformation and increased pinning effect is achieved. Therefore, the hardness property of the welded joint is improved. Generally, the hardness of the welded joint decreased gradually from the SZ to the TMAZ and then to the HAZ [59]. The reason is due to the fact that particle content and the degree of grain refinement decreased in that order in the welded joint.

4.2. *Effects of particle addition on the tensile strength of AA 6061-T6 friction stir welded joint*

Particulate reinforcement addition has been discovered and reported to show some improvements on the tensile properties of FSWed-joint of heat-treatable aluminium alloys, especially AA6061-T6 [7,58,99]. This has been shown to be true for certain volume of particle content/addition. The particle content is often estimated by the size of the groove created along the adjoining line. The center groove width (CGW) of 2 mm and below has been reported to give improved tensile strength while (CGW) beyond this will practical give no improvement due to high volume of particle addition [100]. For example, *Devaraju* et al. [88] reported that higher volume of particles additions in friction stir processed AA 6061-T6

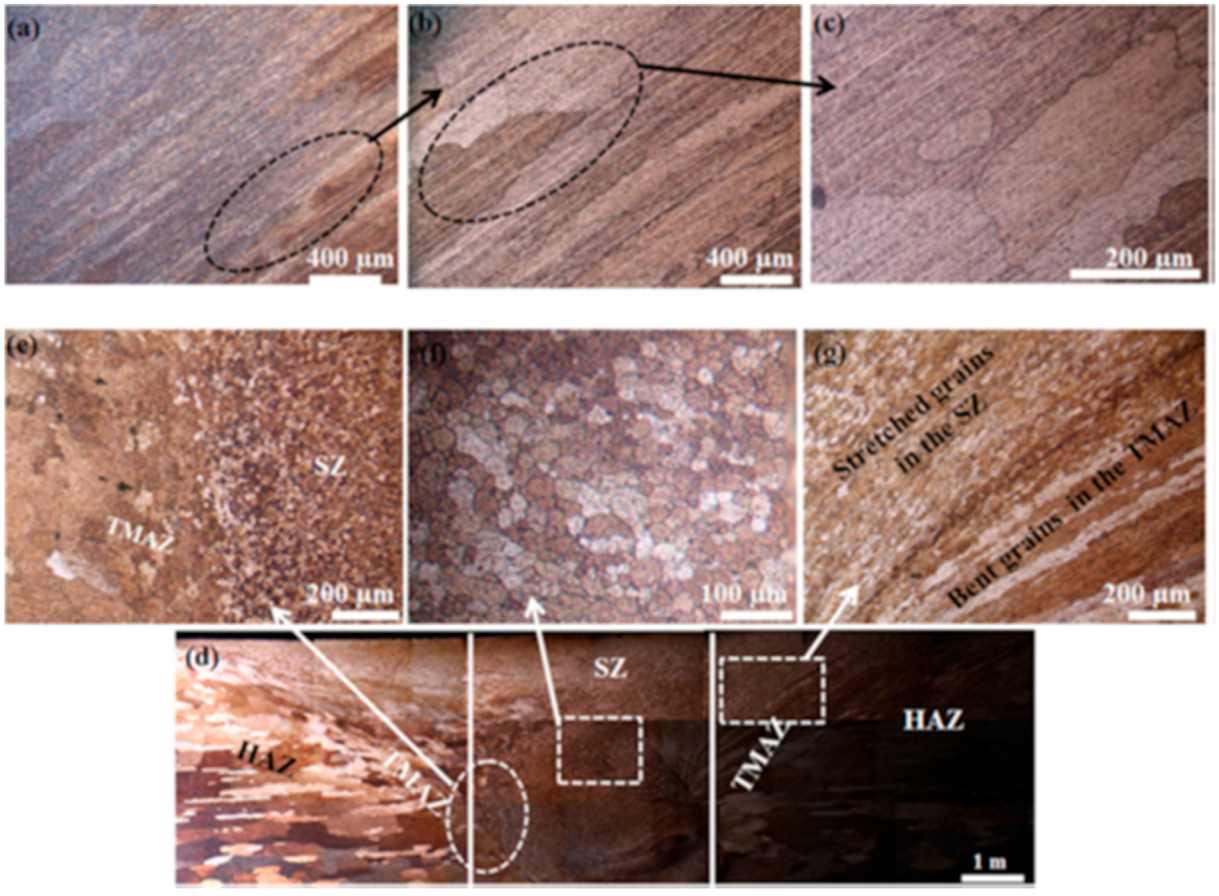

Fig. 17 – Optical micrographs showing the microstructure of (a–c) as received AA 6061-T6 and (d–g) varying zones in the friction stir welded joint [46].

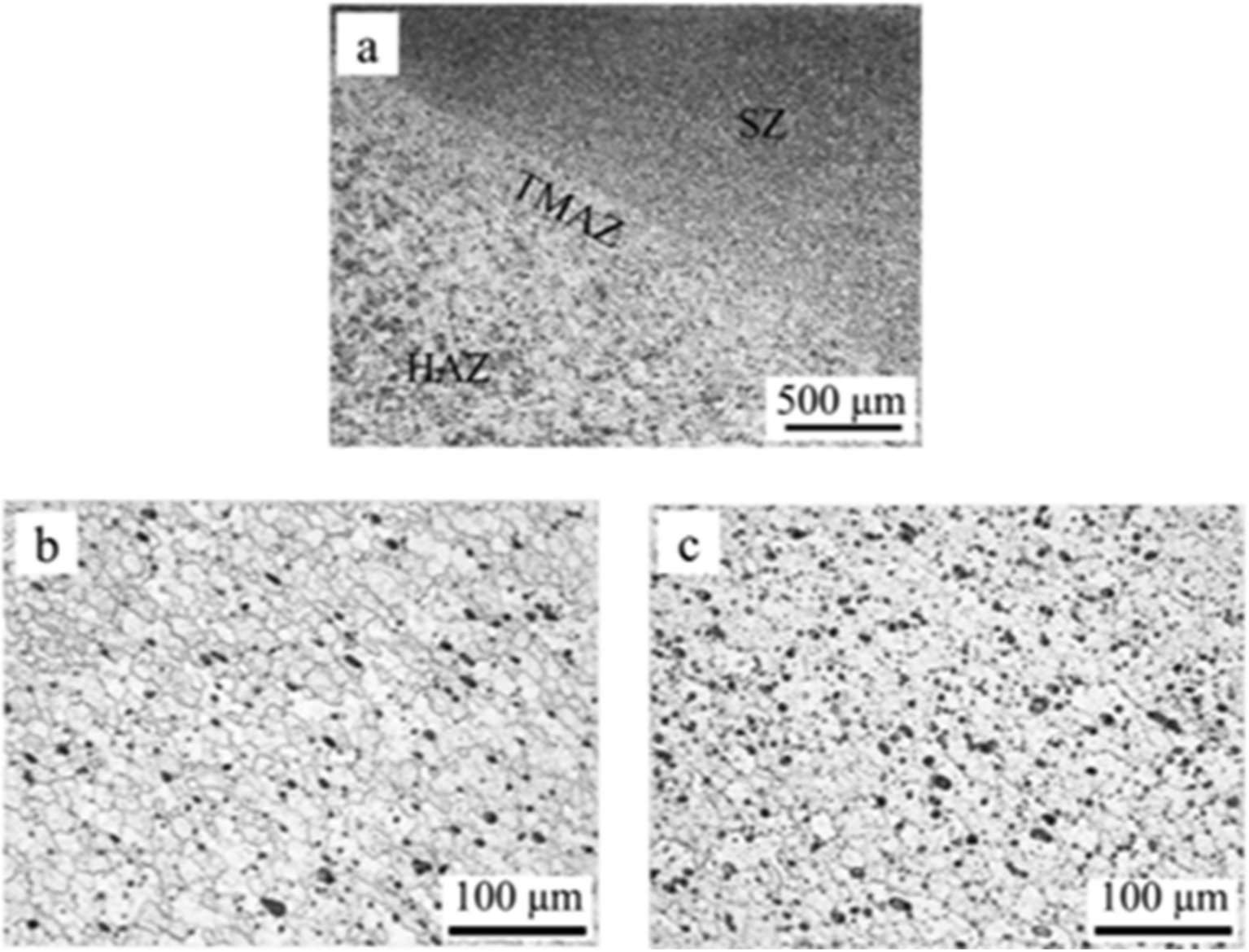

Fig. 18 – Micrographs showing the microstructure of (a) FSW zones and stir zone of friction stir welded joint (b) before and (c) after post–weld heat treatment [4].

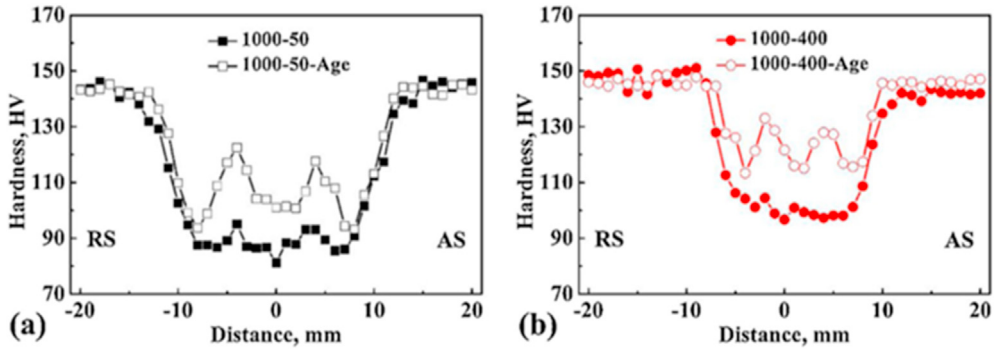

Fig. 19 – Transverse cross-section of Hardness profile of the FSW joints of AA6061-T6 before and after aging with various welding speeds: (a) at 50 mm/min and (b) 400 mm/min [58].

surface resulted in lower ultimate tensile strength (UTS) and joint efficiency compared with friction stir processed surface with lower volume of particles addition. The reason can be attributed to the fact that increasing the percentage by volume of the particles increases the tendency for particle agglomeration or clustering, which often brings about weaker cohesion between the particles and the aluminium matrix [101].

As previously mentioned, significantly low tensile strength around the welded joint is due to loss of structural strengthening in the joint after welding [77]. In the past, additions of reinforcement particles such as SiC [102,103], Al_2O_3 [7], B_4C [58], TiB_2 [104], Cu powder [20,56], graphite [88], graphene and carbon nanotubes (CNTs) [91] have been reported to enhance the strengthening of the welded joint. The incorporation of nano- and micro-sized reinforcement particles initiates pinning effect which often results in substantial refinement of the plastically deformed aluminium matrix during FSW. Also, the particles additions restrict or oppose dislocation motion. These two phenomena (i.e. aluminium matrix refinement and restriction of the dislocation movement) are the reasons for improved tensile strength exhibited by the particle reinforced AA6061-T6 friction stir weldments over the unreinforced. This occurrence is similar to other aluminium alloys. Table 2 gives a summary of the past work on the improvement of mechanical properties including UTS of AA6061-T6 FSWed joints reinforced with various particles under different processing conditions. It is observed that all the listed work in Table 2 used single and at most double weld passes. The reason is to limit the softening effect because increasing the number of weld passes increases the generated frictional heat and causes more dissolution of the strengthening precipitates. Also, key findings in Table 2 show that the reinforced joints exhibited significantly improved hardness and wear properties compared with the unreinforced. Another inference that can be drawn from Table 2 is that the suitable parameters for achieving sound welds of particulate reinforced AA6061-T6 FSWed-joint are usually in the range 600–1400 rpm rotational speed and traverse speed of 30–90 mm/min. Also, the nano sized particles show better improvement than the micro-sized. The reasons for this are that (i) smaller particles are well bonded (i.e. better cohesion) with the aluminium matrix and (ii) the matrix grain refinement due to pinning effect is more pronounced with the smaller-sized particles than the bigger-sized particles.

In a study conducted by Mohan et al. [56], the UTS increased to around 179.34N/mm^2 at 600 rpm with the addition of Cu powder reinforcement and suddenly dropped to 131.99N/mm^2 on increment to 750 rpm as shown in Fig. 11. Generally, the UTS increases with increasing the rotational speed due to increased plastic deformation leading to high degree of DR, which eventually results in enhanced grain refinement. However, the reason for the decline in the case of

Table 4 – Tensile properties of friction stir-welded AA6061-T6 joints subjected to varying heat-treatments [85].

Joints	Yield strength (MPa)	Tensile strength (MPa)	Elongation (%)	Joint efficiency (%)
BM	210	272	26	
AW	110	180	15	66
ST	70	160	11	59
STA	90	170	13	63
AG	130	210	20	77

Note: BM – base metal; AW – As-welded; ST- Solution treated; STA – Solution treated and Aged; AG-artificial aged.

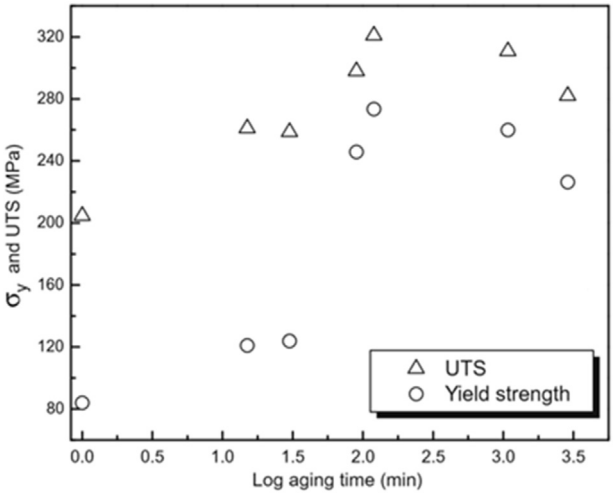

Fig. 20 – Yield and ultimate tensile strengths of friction stir-welded AA6061-T6 joints at varying aging conditions [113].

Table 5 – Some optimum heat treatment conditions established for high quality AA 6061-T6 FSWed-joints.

S/N	Type of FSW	Material	Thickness	Process parameters	Optimum Post–weld heat treatment condition	Microstructural change	Findings	Ref
1	CFSW	AA 6061-T6 with Al2O3 particle addition	6 mm	Rotational speed: 1600 rpm; Welding speed: 25–63 mm/min	Solution treatment at 540 °C for 1 h then aged for 18 h at 180 °C	No significant difference in the grain size of the as -welded and PWHTed joints was observed	The PWHT improved the hardness and wear properties of the joint only at 40 mm/min welding speed. This was due to enhanced particle distribution observed at this welding condition	[44]
2	CFSW	Dissimilar AA 2024-T6 -AA 6061-T6	4 mm	Rotational speed: 1000 rpm; Welding speed: 100 mm/min. Tapered pin with 3.5 mm length	Solution treatment at 520 °C for 1 h together with ageing in the air at 165 °C for 18 h	The grain size of the BM, HAZ, TMAZ and SZ increased after PWHT. Also, precipitated Mg2Si particles in HAZ were observed after PWHT	The joint efficiency increased from 59% to 79% and 83% after heat treatment when the AA 6061-T6 when placed at retreating and advancing side respectively. The hardness of the entire weldment increased after PWHT	[116]
3	High-Speed FSW	AA 6061-T6	0.8 mm	Rotational speed: 8000 rpm; Welding speed: 1500 mm/min	Artifical ageing at 175 °C for 12 h	Increased number of Mg2Si, Al8Fe2Si and Al2CuMg precipitates was observed in the joint after PWHT	After PWHT, the hardness and tensile strength of the weldment increased significantly. A maximum of 90.3% joint efficiency was achieved (using Fe backing plate) after PWHT	[117]
4	CFSW	AA 6082-T6	6 mm	Rotational speed: 950–1140 rpm; Welding speed: 90–150 mm/min	Solution treatment at 470 °C for 30 min and then held for another 30 min after the furnace was switched off. Thereafter, the sample was quenched in water		The solution heat treatment of the as-welded samples improved the UTS by approximately 120%.	[118]
5	Right angle FSW (RAFSW)	AA 6061-T6	6.35 mm	Rotational speed: 3500 rpm; Welding speed: 540 mm/min; Shoulder plunge depth: 6.15 mm	Artifical ageing at 160, 180, 200, 220, 240 °C for various periods from 20 min to 18 h	There is evolution of more precipitates in the joint due to artificial ageing	The joint efficiency of RAFSW samples reaches 90% by artificial aging at 180 °C for 18 h	[119]

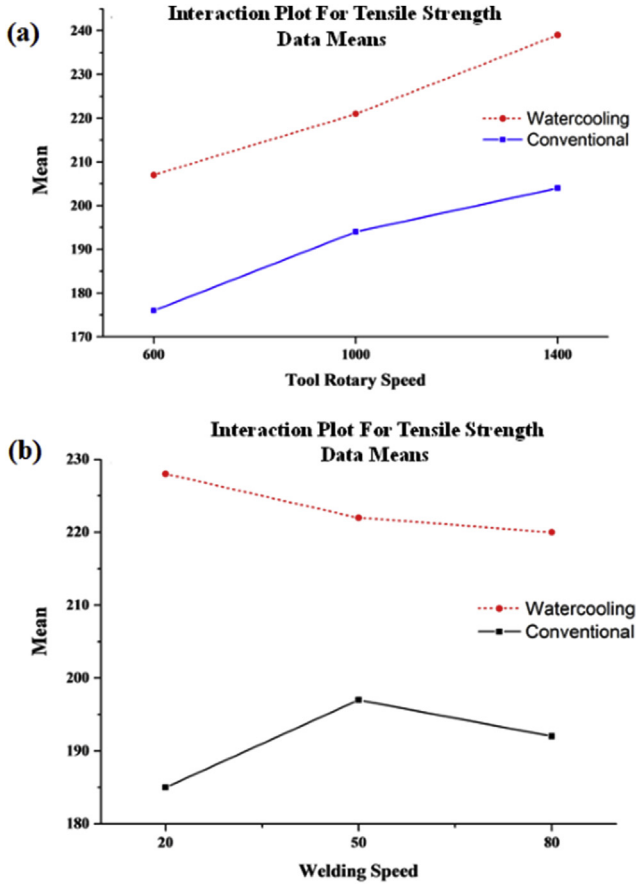

Fig. 21 – Effect of process parameters on the tensile strength of AA6061-T6 FSWed-joints produced at watercooling and no watercooling conditions (a) tool rotational speed (b) travel speed reproduced from [43].

the Cu reinforced joint between 600 and 750 rpm can be attributed to the increased brittleness and fracture tendency of the joint due to the addition of hard Cu particles. Also, addition of the Cu particles may have caused intermetallic compounds formation, which could have also increased the brittleness of the Cu-reinforced joint. According to *Herbert* et al. [92], the UTS also increased with increase in the rotational speed with the addition of particles. UTS of 243 N/mm^2 was realized at 1000 rpm, which later dropped to 204 N/mm^2 with further increase to 1400 rpm (See Table 3).These are all in alignment with the report from *Devaraju* et al. [88] The reason for this is as a result of grain growth and sizes that accompanied the high heat input from increased rotational speed, thereby resulting in deterioration of the UTS at the stir zone. Other reasons attributed to this could be the nature of the reinforcement particles, particles sizes as well as varying processing conditions.

4.3. *Effects of the particle addition on the wear properties of FSWed-Joint of AA6061-T6*

The addition of reinforcement particles has been reported to significantly improve the wear properties of FSWed-aluminium alloys joints such as AA6061-T6 [30]. The wear study of the FSWed-AA6061-T6 joint using SiC, Al_2O_3 and B_4C as reinforcements under 30 N and 50 N loads has been a subject of investigation by *Abioye* et al. [46]. At all load conditions, the entire reinforced joints exhibited significantly lower wear rate compared with the unreinforced joint. The wear volume loss and wear rate increased with the increase in sliding distance (0–1000 m), as shown in Fig. 13. At 30 N load condition, the base metal exhibited the least wear rate while the SiC reinforced joint followed by the Al_2O_3 reinforced joint demonstrated the least wear rate at 50 N load condition (see Fig. 13). According to the report, the higher volume loss and improvements over the base metal at high load is due to increased sliding contact pressure.

Maurya et al. [91] conducted a study on the effect of carbonaceous materials (such as carbon nanotubes (CNTs), graphene (G) and graphite, Gr) on the wear resistance of the friction stir welded joint of AA 6061 (See Fig. 14). It was established that the coefficient of friction (CoF) of the base metal was 0.7 while that of the graphene-, graphite- and carbon nanotubes-reinforced samples are 0.3, 0.51 and 0.53 respectively. The improvement in wear rate shown by the particle-welded samples over the parent metal is associated with grain refinement [106–109], pinning effect of the fine equiaxed grains and DR [11]. Contrary to the findings or

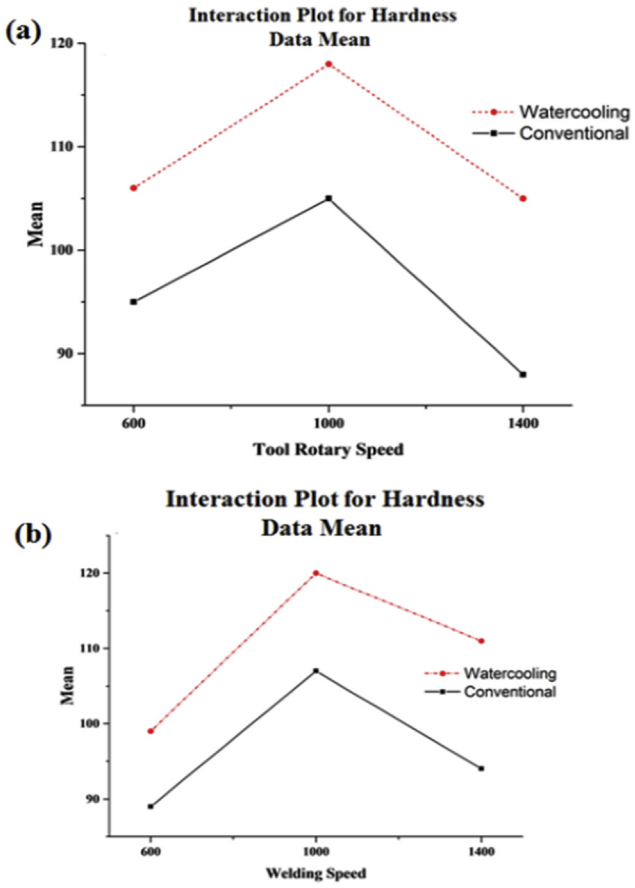

Fig. 22 – Effect of process parameters on the hardness of AA6061-T6 FSWed-joints produced at watercooling and no watercooling conditions (a) tool rotational speed (b) travel speed reproduced from [43].

submissions by *some researchers* [30,46,91], *Singh* et al. [7] found that the Al_2O_3 nanoparticle-reinforced AA6061-T6 joint showed higher weight loss (7.5 mg) than the unreinforced joint (4.1 mg) under pin-on–disk wear test. This is further confirmed by the lower CoF demonstrated by the unreinforced sample, as shown in Fig. 15. This surprising result was attributed to the non-uniform distribution or dispersion of Al_2O_3 nanoparticles within the SZ of the joint [88]. Also, the clustering of the nanoparticles in the HAZ as well as poor interfacial bonding between the accumulated nanoparticles and aluminium matrix was identified as another reason behind the wear behaviour. Increasing the FSW passes or runs could improve the particle distribution which is believed to enhance the (i) particle-aluminium matrix cohesion, (ii) effect of pinning and (iii) cause substantial aluminium matrix grain refinement. All these would lead to a decrement in the wear volume loss and CoF of the reinforced [110]. Generally, particle reinforcement addition contributes remarkably to the wear property improvement as a result of improved hardness and uniform dispersion of particles (micro or nano sized) within the aluminum matrix during FSW [44].

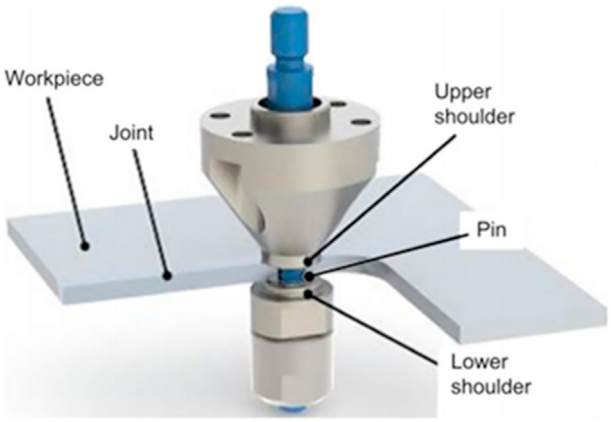

Fig. 23 – A typical bobbin tool FSW set-up [37].

4.4. *Various methods of adding reinforcement particles to the joint*

Moreover, various methods of incorporating reinforcement particles into the FSWed-joints have been utilized by researchers. The most common of these methods is the preparation of a groove on the abutting edges or along the joining direction [21,25,56,88]. Other reported methods include creating a square groove on the surface of the workpiece [91] and drilling an array of cylindrical holes on the faying surfaces or abutting edges of the base materials [7]. So far, groove designs are considered suitable by the respective authors in

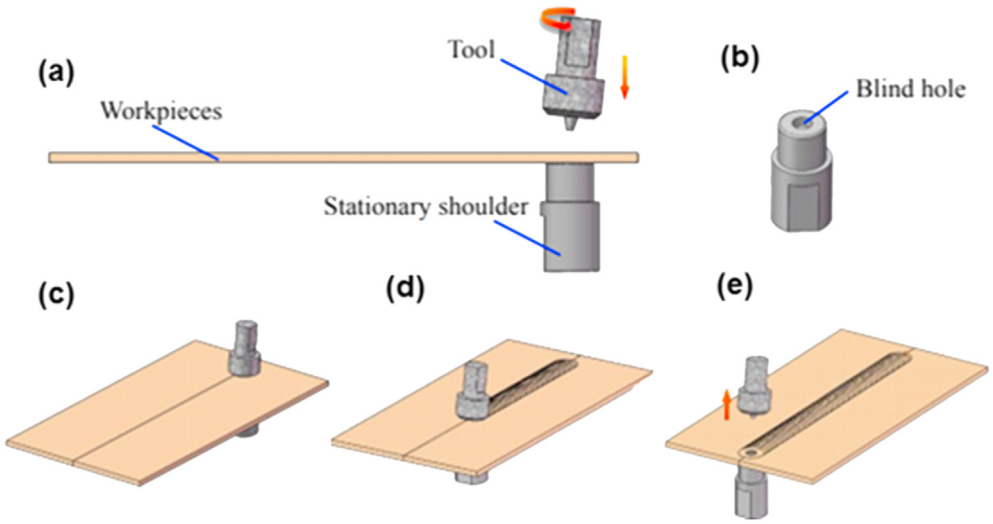

Fig. 24 – Schematic of the PFSW process [35].

order to ensure equal dispersion of particles in the nugget zone [25] as well as prevention of particle scattering during FSW [46].

5. Effects of post weld heat treatment (PWHT) methods

As part of research measures for improving and strengthening the mechanical and wear properties of friction stir butt welded joints of AA6061-T6, post weld artificial aging has turned out to become one of the strategies adopted in achieving these objectives [4,111]. This section will review the effects of post weld artificial aging on the microstructure, hardness, strength and wear properties AA6061-T6 friction stir weldments.

5.1. *Effects of PWHT on the microstructure of AA 6061-T6 friction stir butt weldments*

In order to elucidate the significance of PWHT on the microstructure evolution of the FSWed-joints of AA6061-T6, it is important to understand the morphological characteristics of the as-received aluminium alloy. As illustrated in Figs. 16 and 17, the as-received AA 6061-T6 plate has an elongated structure of inhomogeneous grains. There are also precipitates of Mg_2Si, well dispersed in the aluminium matrix [27]. The different welding zones that make up the FSWed-joint include the nugget or stir zone (SZ), thermo-mechanically affected zone (TMAZ) and the heat affected zone (HAZ), as shown in Fig. 18 (a).

The average grain size of SZ is often smaller than that observed in TMAZ and HAZ due to the varying degrees of DR, plastic deformation and frictional heat input they are subjected to. However, the microstructure of FSWed-joints always appear stretched compared with the as-received AA6061-T6. The stretching which is often due to stirring is usually more pronounced at the SZ and the interface between the SZ and TMAZ (see Fig. 17). Some of the strengthening precipitates dissolve during welding and the remaining fraction retained are unevenly dispersed in the aluminium matrix. According to Baghdadi et al. [4], PWHT has been reported to be responsible for the formation of new precipitates and more homogenous distribution of these strengthening elements in the SZ compared to the SZ of the as-welded sample, as shown in Fig.18b and c. However, it could be deduced from Fig. 18 that the grain size in the SZ of the PWHTed sample is slightly coarser than that of the as-welded sample due to the solutionizing effect.

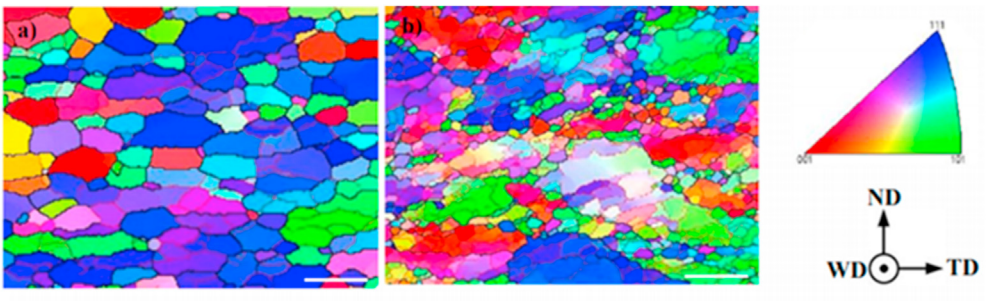

Fig. 25 – EBSD mappings revealing the grain refinement and misorientation distribution in the weld root of (a) PFSW and (b) CFSW joints formed at 300 mm/min [35].

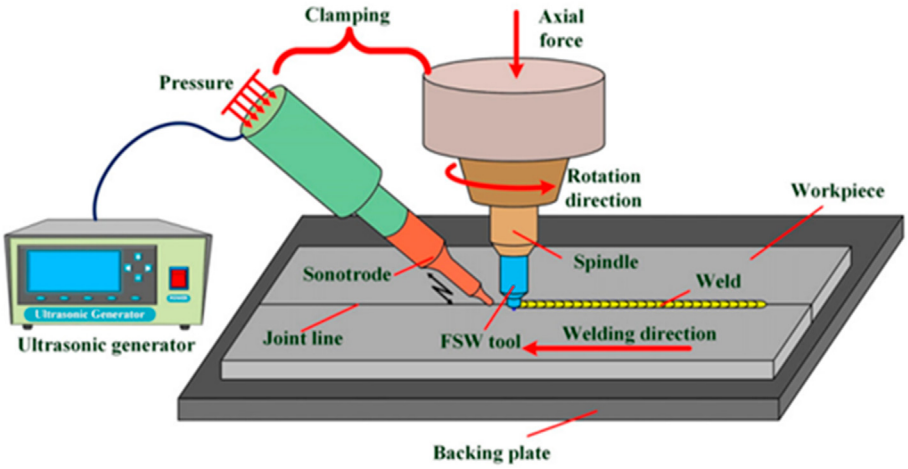

Fig. 26 – A schematic of Ultrasonic assisted FSW process [24].

5.2. *Influence of PWHT on the hardness of friction stir butt welds of AA 6061-T6*

According to literature, the hardness profile of aluminium alloy 6061-T6 becomes altered after FSW as a result of the softening effect experienced in the stir zone (SZ) and thermo-mechanically affected zone (TMAZ). From the studies conducted by [58,111], the hardness profile of the as-welded sample was observed as a bowl shape with the softening area comprising the SZ and TMAZ. The hardness of these softened areas decreased from a value of about 116 HV (T651 base metal) to about 74 HV after FSW. Moreover, the hardness values after PWHT in every zone, increased to about the same values as the aging time and temperature increased. The interpretation of this is that the hardness of the SZ (~74 HV) improved gradually to almost that of the TMAZ (~130 HV) as the as the aging time and temperature increased. It was deduced from this work that after artificial aging, the highest hardness value was observed in the aged specimen with the average hardness of about 130 *VHN*. This was in comparison to the lowest hardness of about 74 *VHN* from the softened area of the as-welded condition as well as the average hardness value of about 116 *VHN* observed in the T651 base metal. This finding is in consistence with that of [58] which also revealed improvement in the stir zone hardness of FSWed-joint of AA6061-T6. It was found that the hardness of the welded joint increased as the traverse speed increased, as presented in Fig. 19.

5.3. *Effects of PWHT on the tensile strength of AA 6061-T6 friction stir butt weldments*

Amongst other established improvement strategies for enhancing the tensile strength of AA6061-T6 welded joints, PWHT has been reported to significantly impact the tensile properties of the aluminium alloy [112]. In a study conducted by [85], the influence of PWHT on the tensile properties of welded joints of AA6061-T6 was carried out on the as-welded (AW) joints, solution treated (ST) joints, solution treated and then aged (STA) joints as well as artificial aged (AG) joints. The results of the various heat treatment methods carried out on the welded joints indicated that the AG sample or joints offered the highest tensile strength as compared to the values obtained for other samples (see Table 4). The ST and STA were found to further reduce the joint strength values when compared to the as-welded joints. This behaviour was attributed to the submission that after conducting solution heat treatment, very few Mg_2Si precipitates remain in the aluminium matrix thereby forming essentially wider precipitate-free zone (PFZ). The wider PFZ is due to further solutionizing of the weld zone which had already been solutionized by the high heat input of the FSW thermal cycle. The UTS of the AG joints achieved in this study was 210 MPa as compared to that of the base metal (272 MPa). This is approximately 20% greater than those of the AW joints. The reason for superior UTS of the AG joints was attributed to finer and uniformly dispersed precipitates observed within the AG welded zone as compared to other heat-treated and as-welded joints. Additionally, the subsequent aging resulted in a substantial increase in precipitate or re-precipitation which led to improvement in the UTS [58].

The natural or artificial aging period also plays a significant role in enhancing the ultimate tensile strength (UTS) of AA6061-T6 welded joints. In a study by Ozturk et al. [113], the UTS was observed to decline with increasing artificial aging time after a peak has been reached (See Fig. 20). Similar findings were reported by Aval and Serajzadeh [114] after prolonged natural aging of AA6061-T6 joints. The report showed that tensile strength decreased considerably after longer aging time. This confirms the finding of Ozturk et al. [113]. Aside the aging time, aging temperature with time also impacts greatly on the tensile properties of AA6061-T6 joints [115]. According to this study, at each aging temperature, it was observed that the tensile strength increased with aging time and reached their peak values. After reaching their peak values, it was reported that the UTS decreased continuously with increasing the aging time and temperature. A summary of some of the established optimum heat treatment conditions for improving the mechanical properties of AA 6061-T6 FSWed-joints is presented in Table 5.

5.4. *Influence of PWHT on wear properties of AA6061-T6 friction stir-welded joints*

Significantly few researches have been conducted on the effect of the post–weld heat treatment on the wear properties of AA 6060-T6 friction stir-welded joints. *Nikoo* et al. [44] investigated the effect of heat treatment on the wear properties of FSWed-joints of AA 6061-T6 reinforced with Al_2O_3 nanoparticles. The outcome of this study revealed that the wear rates of the as-welded (AW) and post weld heat-treated (PWHTed) samples followed similar trend as they increased with increasing the sliding distance. There was no significant improvement in the wear resistance after the PWHT.

5.5. *Impact of water cooling condition on the microstructure and mechanical properties of AA 6061-T6during FSW*

Several comparative investigations have been conducted on the effect of water-cooled friction stir butt welding of aluminium alloys over the natural or air-cooled process [43,64,75,120]. However, some studies have been conducted on the significance of water cooling on the microstructure and mechanical properties of AA6061-T6 during FSW [43,45]. In a study conducted by Fathi et al. [43], it was deduced that irrespective of the welding condition, increase in the rotational speed and traverse speed resulted in a corresponding increase in the tensile strength of welded joint for the conventional process and underwater cooling process. However, the tensile strength of the joint fabricated via water cooling-assisted FSW was remarkably higher than those of joints fabricated via the conventional FSW process (See Fig. 21a and b). The joint strength improvement or efficiency was attributed to the impact of the water cooling process [64]. The induced thermal cycle within the weld nugget during conventional FSW is responsible for the softening or weakening of the HAZ. This causes severe deterioration of the joint strength. According to Ogedengbe et al. [121], failures are often initiated at a point where there is mis-match in properties because this is often the localized point where tensile stress and strains are built up. However, the conduct of FSW in the presence of water cooling condition has been discovered to minimize the thermal cycle thereby increasing the hardness of the HAZ which invariably improves the tensile strength of the weld nugget or joint.

According to Fathi et al. [43], the underwater cooling condition has been reported to cause a significant improvement on the hardness of AA 6061-T6 welded joint as compared to those fabricated by the conventional or natural-cooled FSW. It can be deduced from Fig. 22a and Fig. 22b that as the tool rotational speed and travel speed increases up to 1000 rpm and 50 mm/min respectively, the hardness values of both the water-cooled and conventional welded joints increase respectively before declining. However, in both cases, the water-cooled condition produced welded joints with relatively higher hardness values as compared to those produced via the conventional process. The decrease in hardness after these parametric values was attributed to the microstructural behaviour associated with thermal cycles during the conventional FSW. This resulted in grain formation and grain coarsening within the SZ and HAZ thereby causing a decrease in the hardness [64]. According to *Fathi* et al. [43], when FSW is performed under water cooling, the heat input is moderate or minimized. This tends to prevent the formation of coarse microstructure which results into the uniform distribution of finer grains and thereby enhancing the hardness of the weld nugget.

6. Other variants of FSW

There are some inherent issues associated with the FSW of materials including aluminium alloys. Some of these include kissing bond formation, use of backing plate which limits the FSW flexibility, weld thinning and inability to weld harder materials such as Fe and Ni alloys. In order to overcome these issues, variants of CFSW including bobbin tool FSW, tilt probe penetration FSW, ultrasonic assisted FSW have been developed. These variants are discussed in this section.

6.1. *Bobbin tool FSW*

In CFSW, only the upper shoulder is utilised while the backing plate which supports the workpiece at the base reacts against the down force and prevents occurrence of physical deformation or distortion to the weldments. However, a major disadvantage of CFSW is the insufficient tool penetration, which often results in kissing bond formation and other weld root flaws. Due to the fact that tool stirring is insufficient at the root region of the joint, kissing bond and other root flaws exist. These adversely affect the weld quality. Also, the use of backing plates makes it practically difficult to utilise CFSW in the fabrication of curved profiles and complex shape structures. In an attempt to solve these problems, a new variant of FSW called BTFSW (otherwise termed self-support FSW) has been developed [34,37].

As described in Fig. 23, the arrangement consists of upper and lower shoulders with a pin penetrating through the entire thickness of the workpiece. The pin connects the upper and lower shoulders together. This new arrangement allows for sufficient stirring action from the top to the bottom of the workpiece along the weld joint line. Therefore, kissing bond and other weld root flaws are eliminated in BTFSW. Also, the backing plate has been replaced with the lower shoulder therefore, making the process suitable for the manufacture of complex shaped structures and curved profiles [34]. The main demerit of BTFSW is the high tendency of tool/pin breakage which is enhanced by use of zero tilt angle often utilised in this process [34,35]. The lower shoulder also exerts some residual stress on the pin thus, increasing the tendency of pin breakage. BTFSW of 5-mm-thick 6082-T6 aluminium alloy have been investigated in the past [38] at a rotational speed of 800 rpm, a tilt angle of 4°, and a plunge depth of 0.1 mm. The welding speed was varied from 10 to 200 mm/min. Joints with

no root flaws and kissing bond formation were produced. The UTS and hardness of the BTFSW joints increased with the welding speed and the maximum tensile strength is equivalent to 69% of that of the BM.

6.2. Tilt-probe penetrating FSW (PFSW)

As part of research efforts towards the complete elimination of kissing bond in the root of friction stir welded joints, PFSW has evolved with the development of innovative tool design capable of getting down to the root of weld joint while effectively stirring the plasticized material within the SZ. The arrangement of the PFSW is similar to the BTFSW except that the tilt angle of the upper shoulder is not zero [35]. Apart from high propensity for tool/pin breakage, zero tilt angle in BTFSW often results in deficient material flow in the vertical direction which lowers the weld quality. All these possible defects are eliminated in the PFSW. Fig. 24 shows the set up for PFSW process.

In the past, the microstructure and mechanical properties of 5 mm-thick 2219-T6 aluminium alloy friction stir weldments fabricated via PFSW and CFSW have been investigated by *Hu* et al. [35]. The process parameters include rotational speed of 800 rpm, tilt angle of 2.5° and welding speed of 200–300 mm/min. The results revealed that the joint made via PFSW was sound and without kissing bond and weld root flaws. PFSW sample exhibited maximum UTS of about 354 MPa and elongation of 7.5% which are approximately 79.2% and 58.6% of that of the BM respectively. Compared with a CFSW, PFSW joint exhibited improved mechanical properties.

Fig. 25 shows the EBSD mappings revealing grain structure and misorientation distribution in the root of weld of PFSW and CFSW joints. As seen in Fig. 25a, the PFSW weld joint comprises fine recrystallized grains of average size of 2–3 μm. The interpretation of this is that the material undergoes dynamic recovery and dynamic recrystallization resulting from a severe plastic deformation and friction heat generation during PFSW. As seen in Fig. 25b, the microstructure of the CFSW joint consists of coarse irregular shaped grains mixed with a small number of fine recrystallized grains. The grain size changes from 2 to 3 μm at the top to 15–16 μm at the root of the weld. This is an indication that only some parts of the material experienced DR while the other part (weld root) was not fully stirred due to the limited pin penetration in the workpiece.

6.3. Ultrasonic assisted FSW (UAFSW)

As illustrated in Fig. 26, ultrasonic-assisted FSW (UAFSW) is a variant of FSW where a precursor ultrasonic field is utilised to soften the workpiece along the joint line prior the welding (joining) process [24,122,123]. In the UAFSW set up, the vibrating transducer or vibrator can be positioned in different ways. For example, it can be ahead of the FSW tool, integrated into the rotating tool holder (superimposed), separated from the rotating tool or placed below the workpiece. According to Zhang et al. [122], the ultrasonic transducer can be integrated into the rotating tool holder making the tool to vibrate in the axial direction. With this arrangement, high frequency vibration goes directly to the weld. Also, FSW with ultrasonic vibration placed at the bottom (ahead of the tool position) of the weld has been done by Hu et al. [124]. This was done so that the effect of the vibration is most felt at the weld root where it is believed to be mostly needed. However, the major challenge in placing the vibrator at the bottom of the weld is the positioning/design of the backing plate.

The emergence of this variant overcome the difficulty often encountered in the CFSW of high strength and hard materials such as Fe and Ni alloys [123,124]. Compared with CFSW, UAFSW is more productive, cost-effective and promotes tool life because UAFSW requires not high weld load and can be performed at higher welding speed. Unlike other thermally assisted FSW, UAFSW can cause direct softening of workpiece without much elevation in the process temperature [125,126].This makes the UAFSW produced joint less susceptible to alterations in microstructure which are normally induced by thermal changes. Other advantages of UAFSW include improved material flow, high speed FSW, enhanced grain refinement and improved mechanical properties of the joint. Findings from the past work has established that the microstructure and mechanical properties of UAFSW fabricated joints can be controlled through parametric optimisation and ultrasonic output. Also, it is important to select an appropriate amplitude of vibration to avoid possible defects such as voids and segregation in the weld joint.

Due to the unique advantages it offers, UAFSW has attracted much attentions since its advent [127]. This include parametric optimization [128], experimental investigation and mathematical modelling of temperature fields [129], investigation on the material flow patterns [130], etc. As reported by *Gao* et al. [131] AA6061-T6 joint produced by UAFSW exhibited better strain and grain refinement in the weld nugget zone compared with the one produced via CFSW. This improvement can be traced to the ultrasonic induced complete recrystallization and the fact that ultrasonic vibrations assisted in the recovery of grains is also an advantage [24].

7. Future works

Several attempts have been made on the enhancement of the welded joints of AA60601-T6 during FSW. Some of the adopted research strategies have been reported in this work. However, in order to ensure the sustainability of the strength value of welded joint of AA6061-T6, continuous improvement of the joint properties is critical. Though some variants of FSW such as BTFSW, PFSW and UAFSW have been applied to improve the quality of FSWed-joints of AA6061-T6 and some other aluminium alloys, it is worth investigating the effects of combination of any of these variants (e.g. BTFSW + UAFSW). Also, much work is not available on the application of these variants on friction stir composite welding of AA 6061-T6. Following the existing works on improving the properties and microstructure of the aluminium alloy welded joints, it was observed that much attention was paid towards

experimentation while little or no study has been conducted on numerical investigation of AA 6061-T6 FSWed-joints. Numerical study could be considered for the prediction of the microstructural and mechanical behaviours of welded joints under various welding conditions or parameters of interest. The predicted results are thereafter validated by experimental investigation. Also, scanty recent works exist on pre and post weld heat treatments of reinforced FSWed-joints of AA 6061-T6. Other quenching media apart from water such as spent engine oil, vegetable oils, coconut water, leave and fruit extracts could also be harnessed and adopted in future works.

From economic perspective, the use of synthetic powders or particle reinforcements during FSW has gained so much attention over the years. Most of these particles, such as TiO_2 are expensive and not readily accessible. Hence, for cost effectiveness, priority should be given to the use of industrial ceramic wastes and agro wastes as potential reinforcements for prospective studies.

8. Conclusion and prospects

Excessive heat generation during FSW is responsible for the severe softening and dissolution of the strengthening precipitates of AA6061-T6 butt welded joints. In order to mitigate this challenge, this work presents the various improvement strategies from existing studies which have been established to enhance the joint performance under different processing conditions. These research strategies include parametric optimization, post weld heat treatment methods and particulate reinforcement additions. These adopted strategies are established to impact significantly on the structural strengthening as substantial improvements were reported on the microstructure, tensile strength, hardness and wear properties of the FSWed-joints. As earlier mentioned in this work, high tool rotational speed and low travel speed result in high heat input, which facilitates better material flow around the tool pin and eventually produce severe plastic deformation required to achieve the sound weld joint. Also, the addition of reinforcement particles to the abutting surfaces during FSW gave enhanced mechanical strengthening when compared to the unreinforced weldment. The incorporation of the various nano- and micro-sized reinforcement particles initiates a pinning effect, restriction or opposition to grain boundary dislocation motion and dynamic recrystallization. These characteristics behaviour is responsible for grain refinement, improved tensile strength, hardness and wear properties exhibited by the reinforced welded joint as compared to the unreinforced weldment. Thus, the incorporation of reinforcement particle (of varying sizes) to the friction stir welded joints of AA 6061-T6 significantly enhances the mechanical strengthening of the weldment.

However, from economic perspective, the use of synthetic powders or particle reinforcements during FSW has gained so much attention over the years. Some of these particles, such as TiO_2 are expensive and not readily accessible. Hence, priority should be given to the use of industrial ceramic wastes and agro wastes as potential reinforcements for future works.

Declaration of Competing Interest

The authors declare that they have no known competing financial interests or personal relationships that could have appeared to influence the work reported in this paper.

REFERENCES

[1] Bodunrin MO, Alaneme KK, Chown LH. Aluminium matrix hybrid composites: a review of reinforcement philosophies; mechanical, corrosion and tribological characteristics. Journal of Materials Research and Technology 2015;4(4):434–45.

[2] Thirumoorthy A, Arjunan TV, Senthil Kumar KL. Latest research development in aluminium matrix particulate reinforcement composites- A review. Mater Today: Proceedings. 2018;5:1657–65.

[3] Abioye TE, Zuhailawati H, Aizad S, Anasyida AS. Geometrical, microstructural and mechanical characterization of pulse laser welded thin sheet 5052-H32 aluminium alloy for aerospace applications. Trans Nonferrous Metals Soc China 2019a;29:667–79.

[4] Baghdadi AH, Mohammad Selamat NF, Sajuri Z, Omar MZ. Effect of post-weld heat treatment on the mechanical behavior and dislocation density of friction stir welded Al6061. Mater Sci Eng, A 2019:728–34. https://doi.org/10.1016/j.msea.2019.03.017.

[5] Anas NM, Abioye TE, Anasyida AS, Dhindaw BK, Zuhailawati H, Ismail A. Microstructure, mechanical and corrosion properties of cryorolled-AA5052 at various solution treatment temperatures. Mater Res Express 2020;7(1):1–12.

[6] Gharavi F, Matori KA, Yunus R, Othman NK, Fadaeifarad F. Corrosion behaviour of Al6061 alloy weldment produced by friction stir welding process. Journal of Materials Research and Technology 2015;4(3):314–22.

[7] Singh T, Tiwari SK, Shukla DK. Friction stir welding of AA6061-T6: the effect of Al2O3 nanoparticles addition. Results in Materials 2019;1:1–12. https://doi.org/10.1016/j.rinma.2019.10000 5.

[8] Vysotskiy I, Malopheyev S, Mironov S, Kaibyshev R. Effect of pre-strain path on suppression of abnormal grain growth in friction stir welded 6061 aluminium alloy. Mater Sci Eng, A 2019;760:206–13.

[9] Singh VP, Patel SK, Raryan A, Chen BK. Recent research progress in solid state friction stir welding of aluminium-magnesium alloys: a critical review. Journal of Materials Research and Technology 2020:1–40. https://doi.org/10.1016/j.jmrt.2020.01.008.

[10] Chandran R, Ramaiyan S, Shanbhag AG, Santhanam SKV. Optimization of welding parameters for friction stir lap welding of AA6061-T6 Alloy. Journal of Modern Mechanical Engineering 2018;8:31–41 (Scientific research publishing).

[11] Wang T, Zou Y, Matsuda K. Microstructure and micro-textural studies of friction stir welded AA6061-T6 subjected to different rotational speeds. Mater Des 2015;90:13–21.

[12] Shamin MK. Morphological and structural study of friction stir-welded thin AA6061-T6 Sheets. Int J Mech Eng 2017;6(5):19–24.

[13] Klog O, Grobner J, Wagner G, Schmid-Fetzer R, Eifler D. Microstructural and thermodynamic investigations on friction stir welded Mg/Al-joints. Int J Mater Res 2014;105(2):145–55.

[14] Venkateswaran P, Reynolds AP. Factors affecting the properties of friction stir welds between aluminium and magnesium alloys. Mater Sci Eng 2012;545:26–37.
[15] Singh K, Singh G, Singh H. Review on friction stir welding of magnesium alloys. Journal of Magnesium Alloys 2018;16(4):339–416.
[16] Masoudian A, Tahaei A, Shakiba A, Sharifianjazi F, Mohandesi JA. Microstructure and Mechanical Properties of friction stir weld of dissimilar AZ31-O Magnesium alloy to 6061-T6 aluminium alloy. Transaction of Non-ferrous Metallurgical Society of China 2014;24(5):1317–22.
[17] Zhao Y, Lu Z, Yan K, Huang I. Microstructural characterization and mechanical properties of underwater friction stir welding of aluminium and magnesium dissimilar alloys. Mater Des 2015;65:675–81.
[18] Zhao H, Pan Q, Qin Q, Wu Y, Su X. Effect of processing parameters of friction stir processing on the microstructure and mechanical properties of 6063 aluminum alloy. Mater Sci Eng, A 2019:70–9. https://doi.org/10.1016/j.msea.2019.02.064.
[19] Abioye TE, Olugbade TO, Ogedengbe TI. Welding of dissimilar metals using gas metal arc and laser welding techniques: a review. J Emerg Trends Eng Appl Sci 2017;8(6):225–8.
[20] Garg A, Bhattacharya A. Influence of Cu powder on strength, failure and metallurgical characterization of single, double pass friction stir welded AA6061-AA7075 joints. Mater Sci Eng, A 2019:661–79.
[21] Moradi MM, Aval HJ, Jamaati R. Effect of Pre and Post welding heat treatment in SiC-fortified dissimilar AA6061-AA2024 FSW butt joint. J Manuf Process 2017;30:97–105.
[22] Abioye TE, Mustar N, Zuhailawati H, Suhaina I. Prediction of the tensile strength of aluminium alloy 5052-H32 fibre laser weldments using regression analysis. Int J Adv Manuf Technol 2019b;102(5–8):1951–62.
[23] Abioye TE. The effect of heat input on the mechanical and corrosion properties of AISI 304 arc weldments. Br J Appl Sci Technol 2017;20(5):1–10.
[24] Padhy GK, Wu CS, Gao S. Friction stir-based welding and processing technologies-processes, parameters, microstructures and applications: a review. J Mater Sci Technol 2018;34:1–38.
[25] Jafari H, Mansouri H, Honarpisheh M. Investigation of residual stress distribution of dissimilar Al-7075-T6 and Al-6061-T6 in the friction stir welding process strengthened with SiO2 nanoparticles. J Manuf Process 2019;43:145–53.
[26] Shrivastava A, Krones M, Pfeffekorn FE. Comparison of energy consumption and environmental impact of friction stir welding and gas metal arc welding of aluminium. CIRP Journal of Manufacturing Science and Technology 2015;9:159–68.
[27] Banik A, Barnik SR, Barma JD, Saha SC. An experimental investigation of torque and force generation for varying tool tilt angles and their effects on the microstructure and mechanical properties: friction Stir Welding of AA6061-T6. J Manuf Process 2018;31:395–404.
[28] Kartsonakis IA, Dragotogiannis DA, Koumoulos EP, Karantonis A, Charitidis CA. Corrosion behavior of dissimilar friction stir welded aluminum alloys reinforced with nanoadditives. Mater Des 2016:56–67.
[29] Salih OS, Ou H, Wei X, Sun W. Microstructure and Mechanical Properties of friction stir welded AA6092/SiC metal matrix composites. Mater Sci Eng, A 2019;742:78–88.
[30] Fernandez CMA, Rey RA, Ortega MJC, Verdera D, Vidal CL. Friction stir processing strategies to develop a surface composite layer on AA6061-T6. Mater Manuf Process 2018;33(10):1133–40.
[31] Rathee S, Maheshwari S, Siddiquee AN, Srivastava M. Distribution of reinforcement particles in surface composite fabrication via friction stir processing: suitable strategy. Mater Manuf Process 2018;33(3):262–9. https://doi.org/10.1080/10426914.2017.1303147.
[32] Sinhmar S, Dwivedi DK. Mechanical Behaviour of FSW joint welded by a novel designed stationary shoulder tool. J Mater Process Technol 2020;277:1–9. https://doi.org/10.1016/j.jmatprotec.2019.116482.
[33] Guan M, Wang Y, Huang Y, Lu X, Meng X, Xie M, et al. Non-weld-thinning friction stir welding. Mater Lett 2019;255:1–3. https://doi.org/10.1016/j.matlet.2019.126506.
[34] Li GH, Zhou L, Luo SF, Dong FB, Guo N. Quality improvement of bobbin tool friction stir welds in Mg-Zn-Zr alloy by adjusting tool geometry. J Mater Process Technol 2020;282:1–14. https://doi.org/10.1016/j.jmatprotec.2020.116685.
[35] Hu Y, Liu H, Li S, Du S, Sekulic DP. Improving mechanical properties of a joint through tilt probe penetrating friction stir welding. Mater Sci Eng, A 2018;731:107–18. https://doi.org/10.1016/j.msea.2018.06.036.
[36] Zhang H, Wang M, Zhou W, Zhang X, Zhu Z, Yu T, et al. Microstructure-property characteristics of a novel non-weld-thinning friction stir welding process of aluminum alloys. Mater Des 2015;86:379–87. https://doi.org/10.1016/j.matdes.2015.06.106.
[37] Wang G, Zhao Y, Tang Y. Research progress of bobbin tool friction stir welding of aluminum alloys: a review. Acta Metall Sin 2020;33:13–29. https://doi.org/10.1007/s40195-019-00946-8.
[38] Wan L, Huang Y, Guo W, Lv S, Feng J. Mechanical properties and microstructure of 6082-T6 Aluminum Alloy Joints by self-support friction stir welding. J Mater Sci Technol 2014:1–18. https://doi.org/10.1016/j.jmst.2014.04.009.
[39] Meng X, Huang Y, Cao J, Shen J, Santos JF. Recent progress on control strategies for inherent issues in friction stir welding. Prog Mater Sci 2021;115:1–74. https://doi.org/10.1016/j.pmatsci.2020.100706.
[40] Raturi M, Garg A, Bhaltacharya A. Joint strength and failure studies of dissimilar AA6061-AA7075 friction stir welds: effects of tool pin, process parameters and preheating. Journal of Engineering Failure Analysis 2019;96:570–88.
[41] Kadian AK, Biswas P. Effect of tool pin profile on the material flow characteristics of AA6061. J Manuf Process 2017;26:382–92.
[42] Hakem M, Lebaili S, Mathieu S, Miroud D, Lebaili A, Cheniti B. Effect of microstructure and precipitation phenomenon on the mechanical behaviour of AA6061-T6 aluminium alloy weld. Int J Adv Manuf Technol 2019;102:2907–18. https://doi.org/10.1007/s00170-019-03401-1.
[43] Fathi J, Ebrahimzadeh P, Farasati R, Teimouri R. Friction Stir Welding of aluminum 6061-T6 in the presence of water cooling: analyzing mechanical properties and residual stress distribution. International Journal of Lightweight Materials and Manufacture 2019;2:107–15.
[44] Nikoo MF, Azizi H, Parvin N, Naghibi HY. The influence of heat treatment on microstructure and wear properties of friction stir welded AA6061-T6/Al2O3 Nano composite joint at four different travelling speed. J Manuf Process 2016;22:90–8. https://doi.org/10.1016/j.jmapro.2016.01.003.
[45] Zeng XH, Xue P, Wu LH, Ni DR, Xiao BL, Wang KS, et al. Microstructural evolution of aluminum alloy during friction stir welding under different tool rotation rates and cooling conditions. J Mater Sci Technol 2019;35:972–81.
[46] Abioye TE, Zuhailawati H, Anasyida AS, Yahaya SA, Dhindaw BK. Investigation of the microstructure, mechanical and wear properties of AA6061-T6 friction and

weldments with different particulate reinforcements' addition. Journal of Materials Research and Technology 2019c;8(5):3917–28.
[47] Babu KT, Kumar PK, Muthukumaran S. Mechanical, metallurgical characteristics and corrosion properties of friction stir welded AA6061-T6 using commercial pure aluminium as filler plate. Procedia material science. 3rd international conference on materials processing and characterization, vol. 6; 2014. p. 648–55.
[48] Reimann M, Gartner T, Suhuddin U, Göbel J, dos Santos JF. Keyhole closure using friction spot welding in aluminum alloy 6061-T6. J Mater Process Technol 2016;237:12–8.
[49] Abdulstaar MA, Al-Fadhalah KJ, Wagner L. Microstructural variation through weld thickness and mechanical properties of peened friction stir welded 6061 aluminium alloy joints. Mater Char 2017;126:64–73.
[50] Shamsudeen S, Raja Dhas JE. Optimization of multiple performance characterization of friction stir welded joints with grey relational analysis. J Mater Res 2018;21(6):1–14.
[51] Zhang DQ, Li J, Joo HG, Lee KY. Corrosion properties of Nd:YAG laser–GMA hybrid welded AA6061 Al alloy and its microstructure. Corrosion Sci 2009;51:1399–404.
[52] Mahto RP, Gupta C, Kinjawadekar M, Meena A, Pal SK. Weldability of AA6061-T6 and AISI 304 by underwater friction stir welding. J Manuf Process 2019;38:370–86. https://doi.org/10.1016/j.jmapro.2019.01.028.
[53] Zhang ZW, Li WY, Feng Y, Li JL, Chao YJ. Global anisotropic response of friction stir welded 2024 aluminium sheets. Acta Mater 2015;92:117–25.
[54] Netto N, Tiryakioglu M, Eason P. Characterization of anomalous tool degradation during friction stir processing of 6061-T6 aluminum alloy extrusions: a failure analysis study. Eng Fail Anal 2019;99:1–6.
[55] Tao W, Yong Z, Xuemei L, Matsuda K. Special grain boundaries in the nugget zone of friction stir welded AA6061-T6 under various welding parameters. Mater Sci Eng 2016;671:7–16.
[56] MohanVK, Shamnadh M, Sudheer A. Fabrication and characterization of friction stir welding of AA6061 using copper powder. Mater Today: Proceedings. 2018;5(11):24339–46.
[57]] Abioye TE, Anas NM, Irfan MK, Anasyida AS, Zuhailawati H. Parametric Optimisation for resistance spot welded thin sheet aluminium alloy 5052-H32. Arabian J Sci Eng 2019d;44(9):7617–26.
[58] Li YZ, Zan YN, Wang QZ, Xiao BL, Ma ZY. Effect of welding speed and post-weld aging on the microstructure and mechanical properties of friction stir welded B4Cp/6061Al-T6 Composites. J Mater Process Technol 2019;273:1–11.
[59] Moradi MM, Aval HJ, Jamaati R. Microstructure and mechanical properties in nano and microscale SiC included dissimilar friction stir welding of AA6061-AA2024. Mater Sci Technol 2018;34(4):388–401. https://doi.org/10.1080/02670836.2017.1393976.
[60] Safeen W, Hussain S, Wasim A, Jahanzaib M, Azizi H, Abdall H. Predicting the tensile strength, impact toughness, and hardness of friction stir-welded AA6061-T6 using response surface methodology. Int J Adv Manuf Technol 2016;87:1765–81. https://doi.org/10.1007/s00170-016-8565-9.
[61] Garg A, Raturi M, Bhattacharya A. Strength, failure and microstructure development for friction stir welded AA6061-T6 joints with different tool pin profiles. CIRP Journal of Manufacturing Science and Technology 2020;29:99–114. https://doi.org/10.1016/j.cirpj.2020.03.001.
[62] Goyal A, Rohilla PK, Kaushik AK. Effect of process parameters on the mechanical properties of friction stir welded dissimilar AA6061-T6 and AA5086-H32 Aluminum Alloy joints. Int J Theor Appl Mech 2017;12(1):21–32.
[63] Jayabalakrishnan D, Balasubramanian M. Friction stir weave welding (FSWW) of AA6061 aluminum alloy with a novel tool-path pattern. Aust J Mech Eng 2017;17(3):1–13.
[64] Sinhmar S, Dwivedi DK. Enhancement of mechanical properties and corrosion resistance of friction stir welded joint of AA2014 using water cooling. Mater Sci Eng 2017;684:413–22.
[65] Hamada AS, Jarvenpaa A, Ahmed MM, Jarkari M, Wynne BP, Porter DA, et al. The microstructural evolution of friction stir welded AA6082-T6 aluminium alloy during cyclic deformation. Mater Sci Eng, A 2015;642:366–76.
[66] Zhou L, Li GH, Liu CL, Wang J, Huang YX, Feng JC, et al. Effect of rorational speed on microstructure and mechanical properties of self-reacting friction stir welded Al-Mg-Si alloy. Int J Adv Manuf Technol 2016;89:1–8. https://doi.org/10.1007/s00170-016-9318-5.
[67] Paidar M, Ghavamian S, Ojo OO, Khorram A, Shahbaz A. Modified friction stir clinching of dissimilar AA2024-T3 to AA7075-T6: effect of tool rotational speed and penetration depth. J Manuf Process 2019;47:157–71.
[68] Babu A, Krishna GG. Experimental Investigation of friction stir welding of AA6061 Alloy Joints testing. IOSR J Mech Civ Eng 2015;12(6):1–5.
[69] Elatharasan G, Senthil Kumar VS. An experimental analysis and optimization of process parameter on friction stir welding of AA 6061-T6 aluminium alloy using RSM. Procedia Engineering 2013;64:1227–34.
[70] Leon JS, Jayakumar V. Investigation of mechanical properties of aluminium 6061 alloy friction stir welding. International Journal of Student's Research in Technology and Management 2014;2(4):140–4.
[71] Ramesh Babu KR, Anbumalar V. An experimental analysis and process parameter optimization on AA7075-T6-AA6061-T6 alloy using friction stir welding. Journal of Advanced Mechanical Design, Systems and Manufacturing 2019;13(2):1–10.
[72] Venkatesha BN, Bhagyashekar MS. Preliminary studies on mechanical and metallurgical behavior of friction stir welded butt joints. Procedia engineering. 12th global congress on manufacturing and management, vol. 9; 2014. p. 847–53.
[73] Ravikumar S, SeshagiriRao V, Pranesh RV. Effect of welding parameters on macro and microstructure of friction stir welded dissimilar butt joints between AA7075-T651 and AA6061-T651 Alloys. Procedia Materials Science 2014;5:1726–35.
[74] Ahmed KE, Nagesh BM, Raju BS, Drakshayani DN, Chethan Holla AS. Studies on the effect of welding parameters for friction stir welded AA6082 reinforced with Aluminium Oxide. Mater Today: Proceedings 2020;20:108–19.
[75] Lin H, Wu Y, Liu S, Zhou X. Effect of cooling conditions on microstructure and mechanical properties of friction stir welded 7055 aluminium alloy joints. Mater Char 2018;141:74–85. https://doi.org/10.1016/j.matchar.2018.04.029.
[76] Gomathisankar M, Gangatharan M, Pitchipoo P. A novel optimization of friction stir welding process parameters on aluminium alloy 6061-T6. Mater Today 2018;5(6):14397–404.
[77] He J, Ling Z, Li H. Effect of tool rotational speed on residual stress, microstructure and tensile properties of friction stir welded 6061-T6 aluminium alloy thick plate. Int J Adv Manuf Technol 2015;84:1953–61.
[78] Gadakh VS, Kumar A. Friction stir welding window for AA6061 aluminum alloy. Proceedings of the Institution of Mechanical Engineers. Journal of Engineering Manufacture 2013:1172–81.
[79] Rao CV, Reddy GM, Rao KS. Influence of tool pin profile on microstructure and corrosion behaviour of AA2219 Al - Cu

alloy friction stir weld nuggets. Defence Technology 2015;11:197–208.
[80] Ramulu PJ, Babu AS, Narayanan RG, Prasad SD, Rao PS. The behaviour of friction stir welded (FSW) sheets of AA6061-T6 during in-plane stretching test. International Conference on Design and Manufacturing. Proceedia Engineering 2013;64:862–7.
[81] Akinlabi ET. Effect of shoulder size on weld properties of dissimilar metal friction stir welds. International Journal of Materials Engineering and Performance 2013:1–6. https://doi.org/10.1007/s11665-011-0046-6.
[82] Srivastava AK, Sharma A. Advances in joining and welding technologies for automotive and electronic applications. American Journal of Materials Engineering and Technology 2017;5:7–13.
[83] Reza-E-Rabby M, Reynolds AP. Effect of tool pin thread forms on friction stir weldability of different aluminum alloys. Procedia Engineering 2014;19:637–42.
[84] Abreu Fernandez CM, Rey RA, Cristobal Ortega MJ, Verdera D, Vidal CL. Friction Stir Processing Strategies to develop a surface composite layer on AA6061-T6. Journal of Materials and Manufacturing Processes 2018;33(10):1–9.
[85] Elangovan K, Balasubramanian V. Influences of tool pin profile and tool shoulder diameter on the formation of friction stir processing zone in A6061 aluminium alloy. Mater Des 2008;29:362–73.
[86] Vijayavel P, Balasubramanian V. Effect of pin profile volume ratio on microstructure and tensile properties of friction stir processed aluminum based metal matrix composites. Alloys and Compounds 2017;729:828–42.
[87] Moreira PM, Santos T, Tavares SM, Richter-Trummer V, Vilaça P, De Castro PM. Mechanical and metallurgical characterization of friction stirs welding joints of AA6061-T6 with AA6082-T6. Mater Des 2009;30:180–7.
[88] Devaraju A, Kumar A, Kotiveerachari B. Influence of rotational speed and reinforcements on wear and mechanical properties of aluminum hybrid composites via friction stir processing. Mater Des 2013;45:576–85.
[89] Martin JP. Stationary shoulder friction stir welding. In: Proceedings of the 1st international joint symposium on joining and welding. Osaka, Japan: Woodhead Publishing Limited; November, 2013. https://doi.org/10.1533/9781782421641.477.
[90] Mika DP. Deposition friction stir welding process using filler material and assembly using a die to form a weld profile and prevent flashes. Europian patent application 2006;2:06125031.
[91] Maurya R, Kumar B, Ariharan S, Ramkumar J, Balani K. Effect of carbonaceous reinforcements on the mechanical and tribological properties of friction stir processed Al6061 alloy. Journal of Materials and Design 2016;9(8):155–66.
[92] Khojastehnezhad VM, Pourasl HH. Microstructural characterization and mechanical properties of aluminium 6061-T6 plates welded with copper insert plate (Al/Cu/Al) using friction stir welding. Trans Nonferrous Metals Soc China 2018;28:415–26.
[93] Periyasamy P, Mohan B, Balasubramanian V. Effect of heat input on mechanical and metallurgical properties of friction stir welded AA6061-10% SiCp MMCs. J Mater Eng Perform 2012;21:2417–28.
[94] Asadollahi M, Khalkhali A. Optimization of mechanical and microstructural properties of friction stir spot welded AA 6061-T6 reinforced with SiC nanoparticles. Mater Res Express 2018;5(11):1–45.
[95] Asadi P, Besharati Givi MK, Abrinia K, Taherishargh M, Salekrostam R. Effects of SiC particle size and process parameters on the microstructure and hardness of AZ91/SiC composite layer fabricated by FSP. J Mater Eng Perform 2011;20:1554–62.
[96] Jamalian HM, Ramezani H, Ghobadi H, Ansari M, Yari S, Givi MK. Processing-structure-property correlation in nano-SiC-reinforced friction stir welded aluminium joints. J Manuf Process 2016;21:180–9.
[97] Rajakumar S, Muralidharan C, Balasubramanian V. Predicting tensile strength, hardness and corrosion rate of friction stir welded AA6061-T6 aluminium alloy joints. Mater Des 2011;32:2878–90.
[98] Sahraeinejad S, Izadi H, Haghshenas M, Gerlich AP. Fabrication of metal matrix composites by friction stir processing with different particles and processing parameters. Mater Sci Eng, A 2015;626:505–13.
[99] Asl NS, Mirsalehi SE, Dehghani K. Effect of TiO2 nanoparticles addition on the microstructure and mechanical properties of dissimilar friction stir welded AA6063-T4 aluminium alloy and AZ31B-O magnesium alloy. J Manuf Process 2019;38:338–54.
[100] Baridula RR, Ibrahim AB, Faizal CK, Yahya BC, Kulkarni R, Ramaraju RV. Influence of groove size and reinforcements addition on mechanical properties and microstructure of friction stir welded joints. IOP Conf Ser Mater Sci Eng 2018;319:1–8.
[101] Suresh S, Venkatesan K, Natarajan E. Influence of SiC nanoparticle reinforcement on FSS welded 6061-T6 aluminium alloy. J Nanomater 2018:1–12.
[102] Acharya U, Roy BS, Saha SC. Torque and force perspectives on particle size and its effects on mechanical property of friction stir welded AA6092/17.5SiCp-T6 composite joints. J Manuf Process 2019;38:113–21.
[103] Shokuhfar AA, Cabrera JM, Zhilyaev AP, Omidvar H. In-situ nanocomposite in friction stir welding of 6061-T6 aluminium alloy to AZ31 Magnesium alloy. J Mater Process Technol 2018:296–307.
[104] Singh H, Raina A, Haq I. Effect of TiB2 on the mechanical and tribological properties of aluminium alloys- A review. Mater Today: Proceedings. 2018;5:17982–8.
[105] Herbert MA, Shettigar AK, Nigalye AV, Rao SS. Investigation on microstructure and mechanical properties of friction stir welded AA6061-4.5 Cu-10SiC Composite. IOP Conf Ser Mater Sci Eng 2016;114:1–10.
[106] Abdollahzadeh A, Shokuhfar A, Cabrera JM, Zhilyaev AP, Omidvar H. In-situ nanocomposite in friction stir welding of 6061-T6 aluminium alloy to AZ31 Magnesium alloy. J Mater Process Technol 2018:296–307. https://doi.org/10.1016/j.jmatprotec.2018.08.025.
[107] Zhao Y, Huang X, Li Q, Huang J, Yan K. Effect of friction stir processing with B4C particles on the microstructure and mechanical properties of 6061 aluminium alloy. International Journal of Manufacturing Technology 2015:1–7. https://doi.org/10.1007/s00170-014-6748-9.
[108] Aruri D, Adepu K, Adepu K, Bazavada K. Wear and Mechanical Properties of 6061-T6 aluminium alloy surface hybrid composite [(SiC+Gr) and (SiC + Al2O3)] fabricated by friction stir processing 2013;2(4):362–9.
[109] Thangarasu A, Murugan N, Dunaharan I. Production and wear characterization of AA6082-TiC surface composites by friction stir processing. Procedia Engineering 2014;97:590–7.
[110] Guo JF, Chen HC, Sun CN, Bi G, Sun Z, Wei J. Friction Stir Welding of dissimilar materials between AA6061 and AA7075 Al alloys effects of process parameters. Mater Des 2014;56:185–92.
[111] Boonma J, Khammuangsa S, Uttarasak K, Dutchaneephet J, Boonruang C, Sirikulrat N. Post-weld heat treatment effects on hardness and impact strength of aluminium alloy 6061 friction stir butt weld. Mater Trans 2015;56(7):1072–6.

[112] Ipekoglu G, Erim S, Cam G. Investigation into the influence of post-weld heat treatment on the friction stir welded AA6061 Al-alloy plates with different temper conditions. Metall Mater Trans 2014;45:864–76.
[113] Ozturk F, Sisman A, Toros S, Kilic S, Picu RC. Influence of aging treatment on mechanical properties of 6061 aluminium alloy. Mater Des 2010;31:972–5.
[114] Aval HJ, Serajzadeh S. A study on natural aging behavior and mechanical properties of friction stir welded AA6061-T6 plates. Int J Adv Manuf Technol 2014;71:933–41.
[115] Polat A, Avsar M, Ozturk F. Effects of the artificial aging temperature and time on the mechanical properties and springback behavior of AA6061. Mater Technol 2015;49(4):487–93.
[116] Pabandi HK, Jashnani HR, Pailar M. Effect of precipitation hardening heat treatment on mechanical and microstructure features of dissimilar friction stir welded AA2024-T6 and AA6061-T6 alloy. J Manuf Process 2018;31:214–20. https://doi.org/10.1016/j.jmapro.2017.11.019.
[117] Liu F, Fu L, Chen H. High Speed friction stir welding of ultra-thin AA6061-T6 sheets using different backing plates. J Manuf Process 2018;33:219–77. https://doi.org/10.1016/j.jmapro.2018.05.020.
[118] Azeez S, Mashini M, Akinlabi E. Sustainability of friction stir welded AA6082 plates through post-weld solution heat treatment. Procedia Manufacturing 2019;33:27–34. https://doi.org/10.1016/j.promfg.2019.04.005.
[119] Momeni M, Guillot M. Post-weld heat treatment effects on mechanical properties and microstructure of AA6061-T6 butt joints made by friction stir welding at right angle (RAFSW). Journal of Manufacturing and Materials Processing 2019;42(3):1–13. https://doi.org/10.3390/jmmp3020042.
[120] Mehta KP, Carlone P, Astarita A, Scherillo F, Rubino F, Vora P. Conventional and cooling assisted friction stir welding of AA6061 and AZ31B alloys. Mater Sci Eng, A 2019:252–61.
[121] Ogedengbe TI, Abioye TE, Ekpemogu AI. Investigation of mechanical properties and parametric optimization of the dissimilar GTAW of AISI 304 stainless steel and low carbon steel. World Journal of Engineering 2018;15(5):584–91.
[122] Zhang Z, He C, Li Y, Yu L, Zhao S, Zhao X. Effects of ultrasonic assisted friction stir welding on flow behavior, microstructure and mechanical properties of 7N01-T4 aluminum alloy joints. J Mater Sci Technol 2020;43:1–13. https://doi.org/10.1016/j.jmst.2019.12.007.
[123] Ma Z, Jin Y, Ji S, Meng X, Ma L, Li Q. A general strategy for the reliable joining of Al/Ti dissimilar alloys via ultrasonic assisted friction stir welding. J Mater Sci Technol 2019;35(1):94–9.
[124] Hu Y, Liu H, Fujii H. Improving the mechanical properties of 2219-T6 aluminum alloy joints by ultrasonic vibrations during friction stir welding. J Mater Process Technol 2019;271:75–84. https://doi.org/10.1016/j.jmatprotec.2019.03.013.
[125] Shi L, Wu CS, Liu XC. Modeling the effects of ultrasonic vibration on welding load, temperature and material flow in friction stir welding. J Mater Process Technol 2015;222:91–102. https://doi.org/10.1016/j.jmatprotec.2015.03.002.
[126] Zhong YB, Wu CS, Padhy GK. Effect of ultrasonic vibration on welding load, temperature and material flow in friction stir welding. J Mater Process Technol 2017;239:273–83. https://doi.org/10.1016/j.jmatprotec.2016.08.025.
[127] Eliseev AA, Kalashnikova TA, Gurianov DA, Rubtsov VE, Ivanov AN, Kolubaev EA. Ultrasonic assisted second phase transformations under sever plastic deformation in friction stir welding of AA2024. Materialstoday Communications 2019;21:1–4. https://doi.org/10.1016/j.mtcomm.2019.100660.
[128] Amini S, Amiri M. Study of ultrasonic vibrations' effect on friction stir welding. Int J Adv Manuf Technol 2014;73(1–4):127–35. https://doi.org/10.1007/s00170-014-5806-7.
[129] Shi L, Wu CS, Sun Z. An integrated model for analyzing the effects of ultrasonic vibration on tool torque and thermal processes in friction stir welding. Sci Technol Weld Join 2018;23(5):365–79.
[130] Liu XC, Wu CS. Material flow in ultrasonic vibration enhanced friction stir welding. J Mater Process Technol 2015;225:32–44. https://doi.org/10.1016/j.jmatprotec.2015.05.020.
[131] Gao S, Wu CS, Padhy GK, Shi L. Evaluation of local strain distribution in ultrasonic enhanced Al6061-T6 friction stir weld nugget by EBSD analysis. Mater Des 2016;99:135–44. https://doi.org/10.1016/j.matdes.2016.03.055.

Bamidele T. Ogunsemi is currently a Lecturer I in the Mechanical Engineering Department, College of Engineering, Landmark University, Omu-Aran, Kwara State, Nigeria. He is currently undergoing his PhD program in the Mechanical Engineering Department, Federal University of Technology Akure, Nigeria. His research interests include materials characterization, welding technologies.

Taiwo Ebenezer Abioye completed his PhD from University of Nottingham, UK and undergone his post-doctoral fellowship at Universiti Sains Malaysia, Penang, Malaysia. He is currently a Senior Lecturer in the Department of Industrial and Production Engineering, Federal University of Technology Akure, Nigeria. His research areas include laser materials processing, welding/joining technologies, additive manufacturing, materials characterisation and testing. He has publsihed more than 30 papers in reputed journals (Scopus/ISI indexed) and has been a regular reviewer to many reputed journals.

Tunde Isaac Ogedengbe (PhD) is an Associate Professor in the Department of Mechanical Engineering, Federal University of Technology Akure, Ondo State, Nigeria. He got his PhD from the School of Mechanical, Aerospace and Civil Engineering, University of Manchester, UK. He has great expertise in the optimization of manufacturing processes, welding technologies, engineering design and engineering management. He has published several ISI/Scopus indexed articles in these research areas.

Hussain Zuhailawati is a Professor of Materials Science and Engineering Metallurgy in the School of Materials and Minerals resources Engineering, Universiti Sains Malaysia, Penang, Malaysia. Her fieid of specialisation include fabrication of metal matrix composite using mechanical alloying and powder metallurgy techniques. She is also into metal joining using friction stir welding, resistance spot welding and laser welding techniques. She has published severally in Scopus/ISI indexed journals and has served as editorial board member of many reputed journals.